CAPITAL UNIVERSITY OF SCIENCE AND
TECHNOLOGY, ISLAMABAD

Wave Propagation in Rectangular Waveguide with General Lining Conditions

by

Asma Qamar

A thesis submitted in partial fulfillment for the
degree of Master of Philosophy

in the

Faculty of Computing
Department of Mathematics

2024

I dedicate this effort to my Family, my dear Parents, my elegant Teachers and my supervisor Dr. Muhammad Afzal who are always source of inspiration for me and their contributions are uncounted.

CERTIFICATE OF APPROVAL

Wave Propagation in Rectangular Waveguide with General Lining Conditions

by

Asma Qamar

(MMT213006)

THESIS EXAMINING COMMITTEE

(a)	External Examiner	Dr. Qazi Muhammad Zaigham Zia	COMSATS, Islamabad
(b)	Internal Examiner	Dr. Dur e Shehwar	CUST, Islamabad
(c)	Supervisor	Dr. Muhammad Afzal	CUST, Islamabad

Dr. Muhammad Afzal
Thesis Supervisor
October, 2024

Dr. Muhammad Sagheer
Head
Dept. of Mathematics
October, 2024

Dr. Muhammad Abdul Qadir
Dean
Faculty of Computing
October, 2024

Author's Declaration

I, **Asma Qamar**, hereby state that my MPhil thesis titled "**Wave Propagation in Rectangular Waveguide with General Lining Conditions**" is my work and has not been submitted previously by me for taking any degree from Capital University of Science and Technology, Islamabad or anywhere else in the country/abroad.

At any time if my statement is found to be incorrect even after my graduation, the University has the right to withdraw my MPhil Degree.

(Asma Qamar)

Registration No: MMT213006

Plagiarism Undertaking

I solemnly declare that the research work presented in this thesis is titled "**Wave Propagation in Rectangular Waveguide with General Lining Conditions**" is solely my research work with no significant contribution from any other person. Small contribution/help wherever taken has been dully acknowledged and that complete thesis has been written by me.

I understand the zero tolerance policy of the HEC and Capital University of Science and Technology towards plagiarism. Therefore, I as an author of the above-titled thesis declare that no portion of my thesis has been plagiarized and any material used as reference is properly referred/cited.

I undertake that if I am found guilty of any formal plagiarism in the above-titled thesis even after awarded of MPhil Degree, the University reserves the right to withdraw/revoke my MPhil degree and that HEC and the University have the right to publish my name on the HEC/University website on which names of students are placed who submitted plagiarized work.

(Asma Qamar)

Registration No: MMT213006

Acknowledgement

I got no words to articulate my cordial sense of gratitude to **Almighty Allah** who is the most merciful and most beneficent to his creation.

I also express my gratitude to the last prophet of **Almighty Allah, Prophet Muhammad (PBUH)** the supreme reformer of the world and knowledge for a human being.

I would like to be thankful to all those who provided support and encouraged me during this work.

I would like to be grateful to my thesis supervisor **Dr. Muhammad Afzal**, for guiding and encouraging me in writing this thesis. It would have remained incomplete without his endeavours. Due to his efforts, I was able to write and complete this assertation.

I would like to pay great tribute to my **parents**, for their prayers, moral support, encouragement and appreciation.

Last but not the least, I want to express my gratitude to my **friends** who helped me throughout my MPhil degree.

(Asma Qamar)

Abstract

The primary focus of the current work is on modeling and analyzing the scattering of planar waves with lining conditions. The thesis explores two settings: the first considers lining conditions along the boundaries, while the second incorporates lining conditions embedded in the rigid duct. The governing boundary value problem is addressed using the mode matching technique. This analytical approach involves expanding the wave field in terms of eigenmodes of the waveguide and matching boundary conditions at interfaces to determine the coefficients of the mode expansion. The particular emphasis is on applying the mode-matching method to determine the scattering response at exceptional points. To understanding the behavior of waves on exceptional points have applications in different structural acoustics and heating, ventilation, and air-conditioning (HVAC) systems.

Contents

List of Figures

Abbreviations

BVP	Boundary Value Problem
EP	Exceptional Point
HVAC	Heating, Ventilation and Air conditioning
MM	Mode-Matching

Symbols

c	Speed of sound
C_p	Constant pressure
C_v	Constant volume
k	Wave number
u	Flow velocity
τ	Stress tensor
k	Wave number
α	Transverse wavenumber
g	Gravitational acceleration
p	Instantaneous pressure
p_0	Equilibrium pressure
T	Temperature
ω	Frequency
ϱ	Instantaneous density
ϱ_0	Equilibrium density
r	Specific gas constant
ϱg	Body forces
∇	Divergence
∇_p	Exerting force
γ	Ratio of specific heat
β	Bulk modulus
ψ	Fluid velocity potential
ν	Upper wall parameter
μ	Lower wall parameter

$\hat{Z}$	Impedance
a	Height
η_n	axial wavenumber
δ_{mn}	Kronecker delta

Chapter 1

Introduction and Literature Review

1.1 Introduction

The study of pressure fluctuations in gases, solids, and liquids, including vibrations, falls under the branch of physics known as acoustics. In ancient times, acoustics played a crucial role in managing sound in large public spaces like stadiums, places of worship, and concert halls. However, its scope has expanded significantly in recent times, extending beyond noise control to diverse scientific applications. Acoustics has branched out into specialized fields, including medical acoustics, architectural acoustics, physical engineering acoustics, and musical acoustics, among others.

In today's era, noise-related issues have become a significant concern for researchers and engineers. The primary sources of noise pollution, both indoors and outdoors, stem from HVAC systems in buildings, power stations, vehicles, and other similar sources. Unwanted noise generated by these sources travels through ducts or channels. Thus to minimize this, absorbent materials and specially designed ducts or channels are employed.

This thesis presents an analytical mode-matching approach for modeling the scattering of a plane wave at the interface between a rigid duct and a duct lined with

acoustic material and also explain acoustic waves in a waveguide with a wiremesh embedded in it. The wiremesh can affect the wave propagation and modes in the waveguide, leading to interesting phenomena like waveguide modes, cutoff frequencies, and mode coupling. Helmholtz equations are used to solve the canonical problem with Dirichlet, Neumann or impedance type boundary conditions. The mode-matching technique is used to solve the problem. In quantum physics, exceptional points are unique locations in parameter space where multiple eigenstates merge, leading to a singularity. This phenomenon occurs in dissipative systems, where the non-Hermitian Hamiltonian causes the eigenvalues and eigenvectors to merge, resulting in absorbing properties and behavior [8].

Researchers have long recognized exceptional points, where multiple modes converge, as key to achieve maximum noise attenuation in lined acoustic waveguides. The approach effectively handles mode-matching scheme for the case of no exceptional point and both exceptional points two EP_2 and exceptional points three EP_3 scenarios, where the two-mode and three-mode solutions converge, respectively when K, K' and K'' are zero. The enhanced mode-matching scheme demonstrates numerical robustness and validity, making it a promising tool for adapting to various applications involving complex symmetric operators, with potential for broad applicability.

1.2 Historical Background and Literature Review

This research investigates the behavior of acoustic waves as they travel and scatter within rectangular waveguides or channels, examining their propagation and scattering characteristics. The effectiveness of using acoustical waveguides to reduce unwanted noise can be enhanced by incorporating noise-absorbent materials and introducing nearby reactive liners.

Key features of acoustic scattering in guiding structures with expansions and contractions in geometry play a crucial role in noise reduction applications. For instance, expansion chambers are frequently used to reduce unwanted exhaust noise from internal combustion engines as it travels through the duct. A popular approach for reducing noise in ducts involves adding absorbent coatings or linings to

the interior walls. This poses the challenge of determining the ideal lining design for a given application.

Cremer's idea of optimal attenuation is especially significant in this context. In 1953, Cremer proposed that optimal attenuation occurs when two modes merge into a single mode, a phenomenon known as an exceptional point EP_2, within a lined duct [11]. This phenomenon is not exclusive to acoustic propagation in waveguides, but is a fundamental aspect of non-Hermitian wave physics, as extensively investigated in numerous research studies [7, 19, 29].

Exceptional points also play a crucial role in various phenomena, including the existence of zeros in group velocity, as observed in light waves [13], and instability, as seen in thermoacoustic systems [34], highlighting their importance in understanding complex wave behavior. However, precise mathematical treatment in all these cases requires careful consideration because near an EP, the mathematical framework that governs the scattering process exhibits a manifestation of degeneracy. In situations involving exceptional points, the standard set of eigenmodes lacks completeness, and the usual mathematical framework falls short.

In non-Hermitian physics, exceptional point degeneracy mainly occurs in the scattering matrix, leading to unorthodox phenomena tied to absorption, which demands a more sophisticated mathematical approach to fully understand and describe these effects. Additional understanding of acoustic wave propagation at or near an exceptional point EP is investigated in [9, 15, 17, 20].

In particular, Shenderov (2000) discusses the specific forms of additional wavefunctions needed at EP_2 and EP_3 to guarantee completeness, providing insight into the requirements for a complete basis in the presence of exceptional points [42]. Similar to Jordan's generalized vectors, these functions compensate for the reduced dimensionality in the eigenmode space, effectively restoring the missing dimensions and providing a complete basis for representation. It's noteworthy that at an exceptional point (EP), the additional wavefunctions display peculiar spatial behavior, characterized by either linear growth (EP_2) or quadratic growth (EP_3), distinguishing them from typical wavefunctions [14, 26, 35, 42], which moderates exponential attenuation, though this effect is most significant at larger distances as reported in the source.

The attenuation is not only determined by the source properties, but also by its interaction with additional wavefunctions, which highlights the significant impact of coupling on the attenuation process, as explored in Guo (2020) [15] for acoustic waveguides and Makris et al. (2014) [27] for photonic systems. A crucial aspect of investigating exceptional points EPs is the ability to precisely identify the parameter values that lead to EPs and solve the characteristic equation, enabling a deeper understanding of these phenomena.

Attenuation in acoustic waveguides with lossy wall impedance has been extensively studied due to its significant applications in noise reduction in ducts [30]. The Cremer impedance is a established solution for optimizing mode damping in ducts, and it leads to the formation of an exceptional point where two modes coalesce, resulting in a unique merging of the modal properties [1, 9, 11, 25, 35, 44, 45]. These modes correspond to the two lowest order modes (mode 0 and mode 1), and it is hypothesized that this impedance achieves the highest attenuation for all propagating modes. Recently, dissipative screens have been utilized to filter modes. For instance, radial screens in a circular duct have been implemented to block spinning modes [38]. This approach has also been used for pressure field symmetrization by installing a wire mesh in the middle of a cavity [12].

In this scenario, all non-symmetrical modes are absorbed, while the symmetrical modes are unaffected by the wire mesh.The mode-matching method was employed [24] to analyze sound waves in a three-part duct with porous material attached to the walls. Consequently, the mode-matching method has been employed to address scattering issues in [2–6, 22, 31–33, 41]. In 2012, Lawrie derived a class of orthogonality relations essential for fluid-structure interaction problems [21]. Huang (2002) examined the acoustic behavior of drum-like silencers and sound wave reflection within chambers bounded by vertical plates [16]. In 2019, Satti et al. analyzed the acoustic behavior of expansion chamber silencers with membrane-bounded cavities and horizontal partitions [39]. The splitting walls are assumed to have surfaces that are either rigid, soft, impedance-matched, or sound-absorbing in nature. Rienstra (2003) studied the acoustic modes in a lined channel, both with and without mean flow, and identified three mode types: genuine acoustic modes, acoustic surface waves, and hydrodynamic surface waves [37].

Brambley and Peake (2006) investigated the behavior of surface modes, highlighting the importance of considering viscosity effects and the boundary layer when flow is present [10]. Lawrie and Kirby [23] used this technique for evaluating absorbent silencers. There are two primary methods for modeling finite-length bulk-reacting dissipative silencers, each offering a distinct approach to understanding and analyzing their behavior. One approach is numerical analysis, which typically involves using either the boundary element method [40] or the finite element method [24]. Another approach is to use analytical techniques, which involve calculating the dispersion relation roots and enforcing orthogonality to ensure acoustic field continuity at the silencer's boundaries, thereby determining its acoustic behavior.

Our research on lined acoustic waveguides is structured as follows:

- In **chapter-1**, provide an introduction to the topic, discuss its historical context, and review relevant literature.

- In **chapter-2**, fundamental definitions and key terms related to the subject are defined and explained.

- In **chapter-3**, plane wave propagation with general lining conditions on the bounding walls is discussed.

- In **chapter-4**, plane wave propagation with embedded lining conditions in a rigid duct is explained.

Both the boundary value problems of chapter-3 and chapter-4 are solved by using the mode-matching technique.

- In **chapter-5** provides the summary and concluding remarks of the thesis. References used in the thesis are mentioned in **Bibliography**.

Chapter 2

Preliminaries

The aim of this chapter is to define some basic concepts that are useful to understand the work done in rest of the chapters.

2.1 Waves

A wave is a disturbance that travels through a medium, transferring energy as its particles oscillate back and forth, displacing from one position to another. It's important to understand that waves transfer matter's energy rather than actual matter. Normal waves of sound and light are two examples.

2.2 Types of Wave

Based on the properties of the medium and the energy's transmission, waves can be divided into following three categories.

(i) Mechanical Waves

Waves that require a physical medium to propagate, transferring energy through vibration or oscillation of particles are called mechanical waves. Examples include sound waves, water waves, and vibrations in solids, liquids, and gases.

(ii) Longitudinal Waves

The waves whose propagation direction is parallel to that of the medium's particle orientation are called longitudinal waves. Sound and pressure waves are two examples.

(iii) Transverse Waves

The waves where the particle direction travels perpendicular to the propagation wave direction are called transverse waves.

(iv) Electromagnetic Waves

The waves which are produced when electric and magnetic fields oscillate perpendicular to each other. These waves do not need any physical medium for transfer of energy. Examples include radio waves, microwaves and X-rays.

2.3 Acoustics

Acoustics encompasses the study of how mechanical waves travel through substances. It explores how sound energy is produced, reflected, and transmitted within a medium. Its name originates from the Greek term "akoustikos," meaning related to hearing. The human auditory range typically spans from 20 Hz to 20,000 Hz (20 kHz), with sounds below 20 Hz classified as infrasound and those above 20 kHz classified as ultrasound, both of which are beyond the range of human hearing.

2.4 Acoustic Wave Equation

The acoustic propagation in certain medium can be described mathematically in term of equations, known as acoustic wave equation[18]. This equation can be obtained from the physical laws of motion and equation of state. The derivation is explained in next subsections.

2.4.1 Conservation of Mass

The equation of mass conservation describes the balance between the net flux of mass and the rate of change of mass density, highlighting the fundamental principle of mass conservation in a system [18]

$$\frac{\partial \varrho}{\partial t} + \bigtriangledown.(\varrho u) = 0, \tag{2.1}$$

where u is the velocity of the flow and ϱ is the instantaneous density of mass.

2.4.2 Conservation of Momentum

The momentum conservation equation describes the net rate of momentum transfer to the forces acting on a system, describing how momentum is conserved in the presence of external forces.

$$\frac{\partial(\varrho u)}{\partial t} = - \bigtriangledown .(\varrho u)u - \bigtriangledown p + \varrho g, \tag{2.2}$$

"in which p is the pressure, g is the acceleration due to gravity, $\bigtriangledown p$ denotes the exerting force and ϱg shows the body force. From the above equation,

$$\frac{\partial(\varrho u)}{\partial t} + \bigtriangledown.(\varrho u)u = - \bigtriangledown p + \varrho g, \tag{2.3}$$

which implies that

$$\big(\frac{\partial \varrho}{\partial t} + \bigtriangledown.(\varrho u)\big)u = \varrho\big(\frac{\partial}{\partial t} + u.\bigtriangledown\big)u = - \bigtriangledown p + \varrho g, \tag{2.4}$$

by using the continuity condition, we can write

$$\varrho \frac{Du}{Dt} = - \bigtriangledown p + \varrho g, \tag{2.5}$$

where $\frac{D}{Dt} = \frac{\partial}{\partial t} + u.\bigtriangledown$ is the total time derivative known as Stokes total time derivative [43] contains first term to be time derivative and second term the convective term.

2.4.3 Equation of State

The thermodynamic behaviour of compressible fluid can be defined by the equation of state. For the perfect gas, the equation of state is

$$p = \varrho r T, \tag{2.6}$$

where T used for temperature, and r gives specific gas constant. For a gas enclosed in a vessel of highly thermally conductive walls, the perfect gas isotherm can be given by

$$\frac{p}{p_0} = \frac{\varrho}{\varrho_0}, \tag{2.7}$$

where ϱ_0 and p_0 are the static density and pressure respectively. When no heat loss or gained by the system then perfect adiabatic is

$$\frac{p}{p_0} = \left(\frac{\varrho}{\varrho_0}\right)^{\gamma}, \tag{2.8}$$

where, γ is the ratio of specific heat at constant pressure C_p to the specific heat at constant volume C_v i.e,

$$\gamma = \frac{C_p}{C_v} = \text{Ratio of heat capacities.}$$

The compression and rarefaction in a gas can be defined as condensation i.e

$$s = \frac{\varrho - \varrho_0}{\varrho_0}, \tag{2.9}$$

which yields

$$\varrho = \varrho_0(1 + s). \tag{2.10}$$

By using (2.10) into (2.8) we found

$$\frac{p}{p_0} = (1 + s)^{\gamma}. \tag{2.11}$$

Expanding the right hand side of above equation by using Taylor's series

$$\frac{p}{p_0} = 1 + \gamma s + \frac{\gamma(\gamma-1)}{2fic}s^2 + ... \tag{2.12}$$

For linear relationship

$$\frac{p}{p_0} \approx 1 + \gamma s + O(s^2), \tag{2.13}$$

or

$$\frac{p}{p_0} \approx 1 + \gamma s, \tag{2.14}$$

or

$$p - p_0 = \gamma p_0 s. \tag{2.15}$$

An alternative approach to determine the adiabatic relationship between pressure and density fluctuations involves expanding the pressure as a Taylor series around the equilibrium density can also be written as:

$$p = p(\varrho_0) + (\frac{\partial p}{\partial \varrho})\varrho = \varrho_0(\varrho - \varrho_0) + (\frac{\partial^2 p}{\partial \varrho^2})\varrho = \varrho_0(\varrho - \varrho_0).... \tag{2.16}$$

or

$$p \approx p(\varrho_0) + (\frac{\partial p}{\partial \varrho})_{\varrho=\varrho_0}(\varrho - \varrho_0), \tag{2.17}$$

or

$$p - p_0 = (\frac{\partial p}{\partial \varrho})_{\varrho=\varrho_0}(\varrho - \varrho_0). \tag{2.18}$$

Now comparing equation (2.15) and (2.18) we found

$$\gamma = \frac{\beta}{\varrho}, \tag{2.19}$$

where, $\beta = \varrho_0(\frac{\partial p}{\partial \varrho})_{\varrho=\varrho_0}$, the acoustic pressure at any point can be defined as,

$$P = p - p_0. \tag{2.20}$$

Additionally, Equation (2.18) allows us to define the acoustic pressure as:

$$P = \beta s. \tag{2.21}$$

2.5 Boundary Conditions

The following boundary conditions are defined to model the BVPs:

1. Soft Conditions

2. Rigid Conditions

3. Impedance Conditions

4. Fixed Conditions

5. Free Conditions

2.5.1 Soft Conditions

The soft boundary conditions are Dirichlet's type boundary conditions. In these conditions, the pressure or displacement is taken as zero, i.e.

$$\psi(x_1, y_1) = 0.$$

2.5.2 Rigid Conditions

Neumann's type boundary conditions are actually rigid boundary conditions. In rigid conditions, normal velocity is taken as zero, i.e.

$$\frac{\partial \psi}{\partial x} = 0.$$

2.5.3 Impedance Conditions

The impedance boundary conditions are Robin's type boundary conditions. Robin boundary conditions are combination of Dirichlet boundary conditions and Neumann boundary conditions. These conditions are written as

$$\beta_1 \psi(x_1, y_1) + \beta_2 \frac{\partial \psi(x_1, y_1)}{\partial x_1} = 0,$$

where β_1 and β_2 are arbitrary constants.

2.5.4 Fixed Conditions

In a waveguide, a fixed condition, also known as a "fixed boundary" or "clamped boundary", is a boundary where:

- The displacement (movement) is zero
- The wavefield is not allowed to move or vibrate
- The boundary is rigid and immovable

2.5.5 Free Conditions

In a waveguide, a free condition, also known as a "free boundary" or "unbounded boundary", is a boundary where:

- The wavefield is allowed to move or vibrate freely
- There are no constraints on the displacement (movement)
- The boundary is not rigid or fixed

2.6 Mode-Matching Scheme

Numerous analytical strategies had been developed to investigate the reflection, transmission and absorption of waves in waveguides. The choice of such strategies subjected to material and geometrical properties of the guiding structures as well as the governing system of the physical problem.
Mode-Matching (MM) technique one of the most frequently employed methods

for the problems containing structural discontinuities and different distribution of impedance along the surfaces . This technique is primarily based on the determination of field potentials in segments of guiding structure. Those expansions contain unknown amplitudes. The matching of pressures and velocities at interfaces converts the differential system into linear algebraic systems. Those systems are truncated and solved for the unknown amplitudes.

The applications of physical problems that are manageable by using MM technique are found in automobile industry, heating ventilation and air conditioning systems HVAC of buildings and engineering structures. The key elements in HVAC or automobile industry is a duct like structure. This structure transfer vibrational energy to the environment which is sometime described as noise.
Thus the designs of such elements that help to minimize noise are significant. Sometime these designs involve different geometric variations together with different material properties inside of the structures. The solution of such governing boundary value problems found against the physical problem of interest is not always easy to compute. However the MM technique which is relatively an easy approach gives an interesting method forward to find the solution of such problems. Some of such solutions are explained in next Chapters 3 and 4.

2.7 Basic Definitions

These definitions are taken from[36] and [28].

Waveguide

"A waveguide is a structural component designed to direct waves, including electromagnetic and sound waves, while minimizing energy loss. By constraining the wave expansion to one or two dimensions, the waveguide's geometry plays a crucial role in its functionality. In the context of acoustics, a waveguide behaves similarly to a transmission line, enabling the efficient propagation of sound waves."

Amplitude

"The amplitude of vibration denotes the maximum displacement of a vibrating body from its equilibrium position."

Time Period

"The period of oscillation represents the time taken by the vibrating body to complete one cycle of motion. The period of oscillation is also known as the time period and is denoted by T

$$T = \frac{2\pi}{\omega},$$

where ω is called the circular frequency."

Frequency

"Frequency is defined as the number of times an event occurs per unit of time. It can be denoted by f and can be given as

$$f = \frac{1}{T}, \tag{2.22}$$

where T is time period and f is measured in Hertz."

Chapter 3

Plane Wave Propagation with General Lining Conditions on the Bounding Walls

In this chapter, the problem involving exceptional points considered. The governing problem involves the equation along with rigid and impedance type of BCs. The mode-matching technique is applied to find solution with no exceptional point, two exceptional points and three exceptional points. The chapter is arranged as follows: The description and mathematical formulation of boundary value problem is given in section 3.1. Solution methodology is explained in section 3.2. Standard mode-matching solution is discussed in section 3.3. Enhanced mode-matching solution with two exceptional points is discussed in section 3.4. Enhanced mode-matching solution with three exceptional points is discussed in section 3.5.

3.1 Problem Formulation

A classic problem is examined, where acoustic waves propagate through a two-dimensional waveguide oriented horizontally. The waveguide is composed of two semi-infinite regions, connected at a vertical boundary, and has a height of a units

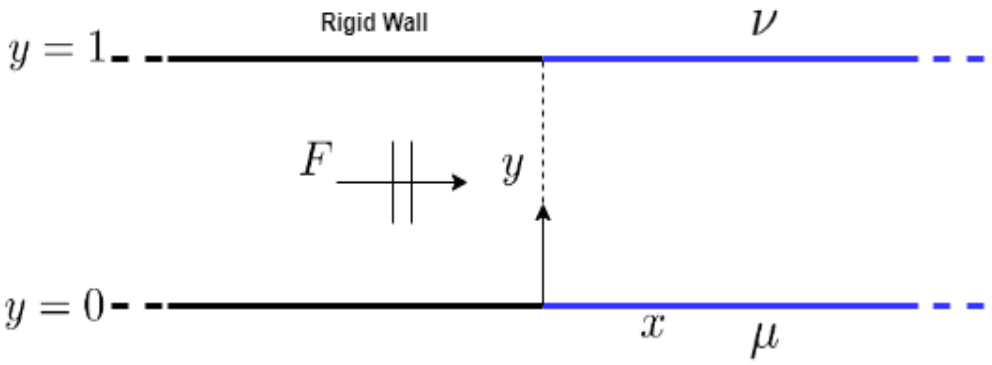

FIGURE 3.1: The physical configuration of waveguide

in a standard Cartesian coordinate system see Fig. 3.1. The waveguide features a junction of two sections with different BCs: one section has rigid walls, while the other section is lined with acoustic material on both walls, creating a mismatch in acoustic impedance at the interface where the two sections meet. The waveguide's lower wall is situated along the axis $\hat{y} = 0$, extending infinitely in the $\hat{x}$ direction $(-\infty < \hat{x} < \infty)$. The interior region of the duct is filled with a compressible fluid, characterized by a density ρ and sound speed c. Note that hat on variable is used to express the dimensional form of variables. The acoustic wave propagation in fluid can be expressed through wave equation

$$\frac{\partial^2 \hat{\Psi}}{\partial \hat{x}^2} + \frac{\partial^2 \hat{\Psi}}{\partial \hat{y}^2} = \frac{1}{c^2} \frac{\partial^2 \hat{\Psi}}{\partial \hat{t}^2}, \tag{3.1}$$

where $\hat{\Psi}$ is fluid potential and the acoustic pressure $\hat{p}$ and velocity $\hat{\mathbf{v}}$ are related to the $\hat{\Psi}$ as $\hat{p} = \rho \frac{\partial \hat{\Psi}}{\partial \hat{t}}$ and $\hat{\mathbf{v}} = \hat{\nabla}\hat{\Psi}$. The waveguide boundaries are rigid and impedance typed. The mathematical form of these boundaries conditions can written from the definition of acoustic impedance $(\hat{Z})$ that is

$$\text{Impedance} = \frac{\text{pressure}}{\text{Normal velocity}}$$

or

$$\hat{Z} = \frac{\hat{p}}{\hat{\mathbf{n}}.\hat{\mathbf{v}}}, \tag{3.2}$$

where $\hat{\mathbf{n}}$ is unit vector directed into the surface, for rigid condition, $\hat{Z}$ is undefined then (3.2) leads to

$$\hat{\mathbf{n}}.\hat{\nabla}\hat{\Psi} = 0. \tag{3.3}$$

Thus at $\hat{x} \leq 0$ for $\hat{y} = 0$, we get the rigid condition from (3.3) as:

$$\frac{\partial \hat{\Psi}}{\partial y} = 0, \quad \hat{y} = 0, 1. \tag{3.4}$$

here, for $\hat{x} \geq \hat{0}$, the impedance condition (3.2) for $y \hat{=} 0$ leads to

$$\hat{Z}\frac{\partial \hat{\Psi}}{\partial y} = \rho\frac{\partial \hat{\Psi}}{\partial \hat{t}}, \quad \hat{y} = 0. \tag{3.5}$$

Likewise, for $\hat{y} = 1$, we get the impedance condition from (3.2) as:

$$\hat{Z}\frac{\partial \hat{\Psi}}{\partial y} = -\rho\frac{\partial \hat{\Psi}}{\partial \hat{t}}, \quad \hat{y} = 1. \tag{3.6}$$

Assuming the harmonic time dependence $e^{-i\omega\hat{t}}$, we can write

$$\left.\begin{aligned} \hat{\Psi}(\hat{x}, \hat{y}, \hat{t}) &= \hat{\psi}(\hat{x}, \hat{y})e^{-i\omega\hat{t}}, \\ \hat{P}(\hat{x}, \hat{y}, \hat{t}) &= \hat{p}(\hat{x}, \hat{y})e^{-i\omega\hat{t}}, \\ \hat{\mathbf{V}}(\hat{x}, \hat{y}, \hat{t}) &= \hat{\mathbf{v}}(\hat{x}, \hat{y})e^{-i\omega\hat{t}}. \end{aligned}\right\} \tag{3.7}$$

By making use of (3.7), we can transform (3.1),(3.4)-(3.6) as:

- Helmholtz equation

$$\left\{\frac{\partial^2}{\partial \hat{x}^2} + \frac{\partial^2}{\partial \hat{y}^2} + \hat{k}^2\right\}\hat{\psi}(\hat{x}, \hat{y}) = 0. \tag{3.8}$$

- Rigid conditions

$$\frac{\partial \hat{\Psi}}{\partial \hat{y}} = 0, \quad \hat{y} = 0, 1. \tag{3.9}$$

- Impedance conditions

$$\hat{Z}\frac{\partial \hat{\Psi}}{\partial y} = -i\omega\rho\hat{\psi}, \quad y = 0, \tag{3.10}$$

$$\hat{Z}\frac{\partial \hat{\Psi}}{\partial y} = i\omega\rho\hat{\psi}, \quad y = 1. \tag{3.11}$$

We make the problem dimensionless using transformation

$$\left.\begin{aligned} \hat{x} &= ax, \\ \hat{y} &= ay, \\ w\hat{t} &= t, \\ a^2\hat{\psi} &= \psi. \end{aligned}\right\} \tag{3.12}$$

By using transformation (3.12), the dimensionless form (3.8) and boundary condition from (3.9)-(3.11) are

$$\left\{\frac{\partial^2}{\partial x^2} + \frac{\partial^2}{\partial y^2} + k^2\right\}\psi(x,y) = 0, \tag{3.13}$$

The wave number k is normalized as $k = \hat{k}a$, and the fluid velocity potential is represented by the dimensionless function $\psi(x,y)$, which has the following form:

$$\psi(x,y) = \begin{cases} \psi_1(x,y) & ,0 \le y \le 1, x < 0 \\ \psi_2(x,y) & ,0 \le y \le 1, x > 0. \end{cases}$$

The portion of the duct extending from $x = 0$ to the left $x < 0$ features rigid walls, which are characterized by the following BCs:

$$\frac{\partial \psi_1}{\partial y} = 0, \quad y = 0 \quad \text{and} \quad 1, \quad x < 0. \tag{3.14}$$

The duct section located in the region $x > 0$ is lined with acoustic material, and the following BCs apply in this local region:

$$\frac{\partial \psi_2}{\partial y} + \mu\psi_2 = 0 \quad \text{at} \quad y = 0. \tag{3.15}$$

and

$$\frac{\partial \psi_2}{\partial y} - \nu\psi_2 = 0 \quad \text{at} \quad y = 1, \tag{3.16}$$

where

$$Z_\mu = \frac{ic\rho\hat{k}a}{\mu},$$

and

$$Z_\nu = \frac{ic\rho\hat{k}a}{\nu},$$

The dimensionless wall admittance is defined in terms of the complex acoustic impedance, Z_μ and Z_ν.

3.2 Solution Methodology

The boundary value problem defined in (3.13)-(3.16) can be solved by using the mode matching technique. Due to the involvement of lined boundary [25] conditions there exist exceptional points and there will exist standard and enhanced mode matching formulation in solution procedure. For the modelled problem Lawrie and Debain [25] have found two and three exceptional points. Thus, the three formal action of solution are possible for the modelled setting.

- Standard Mode-Matching Solution
- Enhance Mode-Matching with Two Exceptional Points
- Enhance Mode-Matching with Three Exceptional Points

These solution are explained in sections.

3.3 Standard Mode-Matching Solution

The standard mode-matching form does not involve any exceptional point. For standard mode-matching we determine eigenfunction expansions by using separation of variable method. For region $x \leq 0$, the governing equation and rigid boundary condition are

$$\frac{\partial^2 \psi_1}{\partial x^2} + \frac{\partial^2 \psi_1}{\partial y^2} + k^2 \psi_1 = 0, \tag{3.17}$$

$$\frac{\partial \psi_1}{\partial y} = 0, \quad y = 0, \tag{3.18}$$

and

$$\frac{\partial \psi_1}{\partial y} = 0, \quad y = 1. \tag{3.19}$$

For separation of variable method we assume

$$\psi_1 = X_1(x)Y_1(y). \tag{3.20}$$

On using (3.20) into (3.17), we get

$$k^2 + \frac{Y_1''}{Y_1} = -\frac{X_1''}{X_1} = \eta^2(\text{say}), \tag{3.21}$$

which on solving yields

$$Y_1 = c_1 \cos(\tau y) + c_2 \sin(\tau y) \tag{3.22}$$

and

$$X_1 = c_3 e^{i\eta x} + c_4 e^{-i\eta x}. \tag{3.23}$$

where $\eta = \sqrt{k^2 - \tau^2}$ and c_1, c_2, c_3 and c_4 are arbitrary constants. Substituting (3.20) into (3.18) and (3.19) and then making use of (3.21), we get

$$Y_1 = Y_{1n} = \cos \tau_n y, \tag{3.24}$$

where $\tau_n = n\pi$; $n = 0, 1, 2, 3, \cdots$. Further, at Y_{1n}; $n = 0, 1, 2, 3, \cdots$. are orthogonal and satisfy the orthogonality relation

$$\int_0^1 Y_{1n} Y_{1n} dy = \delta_{mn} E_n, \tag{3.25}$$

where

$$E_n = \int_0^1 Y_{1n}^2 dy. \tag{3.26}$$

Note that for $\tau_n = n\pi$; $n = 0, 1, 2, 3, \cdots$. are infinite many solutions and superposition principle can be applied ti formulate the eigenfunction expansion as:

$$\psi_1 = \sum_{n=0}^{\infty} F_n Y_{1n}(y) e^{i\eta_n x} + \sum_{n=0}^{\infty} A_n Y_{1n}(y) e^{-i\eta_n x}. \tag{3.27}$$

Whereas, if we consider the fundamental duct mode to be the incident then we choose $F_n = F\delta_{no}$, then (3.27) takes formulation

$$\psi_1 = Fe^{ikx} + \sum_{n=1}^{\infty} A_n Y_{1n} e^{-i\eta_n x}. \tag{3.28}$$

where A_n is a complex number that describes the amplitude and phase of the nth mode that is reflected at the interface between the two sections of the duct. This term (3.28) is likely the incident wave that is interacting with the interface between the two sections of the duct, and F is a constant that characterizes the strength of the incident wave. The dimensionless axial wavenumbers η_n are defined by the equation $\eta_n = \sqrt{k^2 - n^2\pi^2}$ for integer values of $n = 0, 1, 2, \cdots$. Notably, when x equals 0, the eigenfunction expansion simplifies to Fourier cosine series.
For region $x \geq 0$, we have governing equation and BCs are:

$$\frac{\partial^2\psi_2}{\partial x^2} + \frac{\partial^2\psi_2}{\partial y^2} + k^2\psi_2 = 0, \tag{3.29}$$

$$\frac{\partial\psi_2}{\partial y} + \mu\psi_2 = 0, \quad y = 0, \tag{3.30}$$

and

$$\frac{\partial\psi 2}{\partial y} - \nu\psi_2 = 0, \quad y = 1. \tag{3.31}$$

For separation of variable method we assume

$$\psi_2 = X(x)Y(y). \tag{3.32}$$

On using (3.32) into (3.29), we get

$$\frac{Y''}{Y} + k^2 = -\frac{X''}{X} = s^2(\text{say}), \tag{3.33}$$

which on solving yields

$$Y = c_5\cos(\alpha y) + c_6\sin(\alpha y), \tag{3.34}$$

and

$$X = c_7 e^{isx} + c_8 e^{-isx}, \tag{3.35}$$

where $s = \sqrt{k^2 - \alpha^2}$ and c_5, c_6, c_7 and c_8 are arbitrary constants. To find these we rewrite (3.30) and (3.31) using (3.32) as:

$$Y' + \mu Y = 0, \quad y = 0, \tag{3.36}$$

and

$$Y' - \nu Y = 0, \quad y = 1, \tag{3.37}$$

by substituting (3.34) into (3.36), we get $c_6 = -\dfrac{\mu}{\alpha}$ which on using into (3.34) leads to the following form

$$Y = \left(\cos(\alpha y) - \frac{\mu}{\alpha}\sin(\alpha y)\right). \tag{3.38}$$

Now using (3.35) into (3.37), we get

$$(\mu + \nu)\cos\alpha + (\alpha - \frac{\mu\nu}{\alpha})\sin\alpha = 0. \tag{3.39}$$

If we defined

$$\mu + \nu = q,$$

and

$$\mu\nu = p.$$

Then (3.39) can be written as:

$$K(s) = q\cos\alpha + (\alpha - \frac{p}{\alpha})\sin\alpha, \tag{3.40}$$

here $\alpha = \sqrt{k^2 - s^2}$ are the roots of (3.40) and can be found numerically. where

$$\alpha_n = n\pi\left[1 - \frac{q}{(n\pi)^2} + \frac{q^3/3 - q^2 - pq}{(n\pi)^4} + \cdots\right], \quad \text{as} \quad n \to \infty,$$

The expression provides a good estimate when the values of p and q are moderate for $n = 1, 2, 3, \cdots$. As there can be infinite many values of α, for which (3.40) holds then the eigenfunction expansion can be given as:

$$\psi_2 = \sum_{n=1}^{\infty} B_n Y_n(y) e^{(is_n x)} + \sum_{n=1}^{\infty} C_n Y_n(y) e^{(-is_n x)}. \tag{3.41}$$

As there is no neglection in region at $x \geq 0$, thus $c_n = 0$ and (3.41) takes formulation

$$\psi_2 = \sum_{n=0}^{\infty} B_n Y_n(y) e^{(is_n x)} \tag{3.42}$$

Note that $Y_n(y)$ are orthogonal and fulfill the following orthogonality relation

$$\int_0^1 Y_m(y) Y_n(y) dy = \delta_{mn} P_n, \tag{3.43}$$

where

$$P_n = \int_0^1 Y_n^2(y) dy. \tag{3.44}$$

Now A_n, B_n are unknowns. To find these unknowns we use matching condition.

Now we check continuity conditions at $x = 0$

Continuity of Pressure

$$\psi_1(0, y) = \psi_2(0, y) \quad 0 < y < 1. \tag{3.45}$$

Now using (3.45) in (3.28) and (3.42), we get

$$F + \sum_{n=0}^{\infty} A_n \cos(n\pi y) = \sum_{n=1}^{\infty} B_n Y_n(y). \tag{3.46}$$

Multiplying (3.46) with $\cos(m\pi y)$ and integrating from 0 to 1.

$$\begin{aligned} &F \int_0^1 \cos(m\pi y) dy + \sum_{n=0}^{\infty} A_n \int_0^1 \cos(m\pi y) \cos(n\pi y) dy \\ &= \sum_{n=1}^{\infty} B_n \int_0^1 \cos(m\pi y) Y_n(y) dy. \end{aligned} \tag{3.47}$$

Using the standard orthogonality property of cosine functions, we can determine the coefficients A_m by exploiting the orthogonality relationship.

$$F\delta_{m_0} + \sum_{n=0}^{\infty} A_n \delta_{mn} \frac{\epsilon_m}{2} = \sum_{n=1}^{\infty} B_n L_{mn}, \tag{3.48}$$

which on simplification leads to

$$A_m = \frac{-2F\delta_m 0}{\epsilon_m} + \frac{2}{\epsilon_m} \sum_{n=1}^{\infty} B_n L_{mn}, \tag{3.49}$$

where $\epsilon_n = 2$, if $n = 0$ and $n = 1$ otherwise here

$$L_{mn} = \int_0^1 Y_n(y) \cos m\pi y dy. \tag{3.50}$$

Continuity of normal velocity

$$\psi_{2x}(0, y) = \psi_{1x}(0, y). \tag{3.51}$$

By using (3.28) and (3.42) in (3.51), we get

$$i \sum_{n=1}^{\infty} B_n s_n Y_n = ikF - i \sum_{n=0}^{\infty} A_n \eta_n \cos(n\pi y). \tag{3.52}$$

Multiply (3.52) with $Y_j(y)$ and integrate 0 to 1

$$\sum_{n=1}^{\infty} B_n s_n \int_0^1 Y_n Y_j dy = kF \int_0^1 Y_j dy - \sum_{=0}^{\infty} A_n \eta_n \int_0^1 Y_j \cos(n\pi y), \tag{3.53}$$

using (3.43) and(3.50) into (3.53), we get

$$\sum_{n=1}^{\infty} B_n s_n \delta_{jn} P_j = KFL_{0j} - \sum_{n=1}^{\infty} A_n \eta_n L_{nj}, \tag{3.54}$$

which on simplification leads to

$$B_j = \frac{kFL_{0j}}{s_j P_j} - \frac{1}{s_j P_j} \sum_{n=1}^{\infty} A_n \eta_n L_{nj}, \quad j \geq 1. \tag{3.55}$$

On combining (3.49) and (3.55),

$$B_j = \frac{2kFL_{0j}}{s_j P_j} - 2\sum_{n=0}^{\infty} \frac{B_n}{s_j P_j} \sum_{m=0}^{\infty} \frac{\eta_m}{\epsilon_m} L_{mj} L_{mn}. \tag{3.56}$$

For $J \geq 1$

$$B_j \sqrt{s_j P_j} = \frac{2kFL_{0j}}{\sqrt{s_j P_j}} - 2\sum_{n=0}^{\infty} \frac{b_n}{\sqrt{s_n P_n}} \frac{1}{\sqrt{s_j P_j}} \sum_{m=0}^{\infty} \frac{\eta_m}{\epsilon_m} L_{mj} L_{mn}, \tag{3.57}$$

which leads to

$$b_j = \frac{2kFL_{0j}}{\sqrt{s_j P_j}} - 2\sum_{n=0}^{\infty} b_n S_{jn}, \quad j \geq 1, \tag{3.58}$$

where

$$S_{jn} = \frac{1}{\sqrt{s_j s_n P_j P_n}} \sum_{m=0}^{\infty} \frac{\eta_m}{\epsilon_m} L_{mj} L_{mn}, \tag{3.59}$$

and $b_n = B_n \sqrt{s_n P_n}$, $n = 1, 2, 3, \cdots$.

3.4 Enhanced Mode-Matching Solution with Two Exceptional Points

An exceptional point (EP) occurs when there exists a specific value of α_n such that both the functions $k(s_n)$ and $k'(s_n)$ simultaneously vanish, i.e., $k(s_n) = k'(s_n) = 0$. At an exceptional point, the eigenfunctions $Y_n(y) = Y(s_n, y)$ can be used to define a new wave function by differentiating with respect to the parameter s, following the approach outlined in references [35, 42]. This is represented mathematically as:

$$\psi EP_2 = \frac{\partial (Y e^{isx})}{\partial s} = (Y' + ixY) e^{isx}. \tag{3.60}$$

By differentiating Y with respect to $'s'$ we get

$$\frac{\partial Y}{\partial s} = \frac{\partial}{\partial \alpha} [\cos(\alpha y) - \frac{\mu}{\alpha} \sin(\alpha y)] \frac{\partial \alpha}{\partial s}, \tag{3.61}$$

which on simplification we get

$$\frac{\partial Y}{\partial s} = \frac{sy}{\alpha \sin \alpha y} + \frac{sy\mu}{\alpha^2 \cos(\alpha y)} - \frac{s\mu}{\alpha^3 \sin(\alpha y)}, \tag{3.62}$$

and it is easy to see that

$$\frac{\partial}{\partial s}[(\nu Y - \frac{\partial Y}{\partial y})e^{isx}]y = 1 = (\nu\psi EP_2 - \frac{\partial \psi}{\partial y}EP_2)y = 1 = (K' + ixK)e^{isx}. \tag{3.63}$$

Corresponding to any given transverse wavenumber $\bar{\alpha}$, there exists a unique set of wall parameters p, q that satisfy the equation $K(s) = 0$, which can be obtained by using equation (3.40), we get

$$q \cos \bar{\alpha} + (\bar{\alpha} - \frac{p}{\bar{\alpha}}) \sin \bar{\alpha} = 0. \tag{3.64}$$

Now using value of p and q into (3.64), we get

$$(\bar{\mu} + \bar{\nu}) \cos \bar{\alpha} + (\bar{\alpha} - \frac{\bar{\mu}\bar{\nu}}{\bar{\alpha}}) \sin \alpha) = 0, \tag{3.65}$$

which on simplification we get

$$(\bar{\mu} + \bar{\nu}) = -(\bar{\alpha} - \frac{\bar{\mu}\bar{\nu}}{\bar{\alpha}}) \tan \bar{\alpha}. \tag{3.66}$$

Now to find out $\bar{\mu}\bar{\nu}$ taking derivative of (3.40), we get

$$K'(s) = \frac{\partial}{\partial s}\left(q \cos \bar{\alpha} + (\bar{\alpha} - \frac{p}{\bar{\alpha}}) \sin \bar{\alpha}\right).$$

Now using $K'(s) = 0$

$$-q \sin \bar{\alpha} + (1 + \frac{p}{\bar{\alpha}^2}) \sin \bar{\alpha} + (\bar{\alpha} - \frac{p}{\bar{\alpha}}) \cos \bar{\alpha} = 0, \tag{3.67}$$

using values of p and q into (3.67), we get

$$-(\bar{\mu} + \bar{\nu}) \sin \bar{\alpha} + (1 + \frac{\bar{\mu}\bar{\nu}}{\bar{\alpha}^2}) \sin \bar{\alpha} + (\bar{\alpha} - \frac{\bar{\mu}\bar{\nu}}{\bar{\alpha}}) \cos \bar{\alpha} = 0. \tag{3.68}$$

Using (3.66) in (3.68), we get

$$(\bar{\alpha} - \frac{\bar{\mu}\bar{\nu}}{\bar{\alpha}})\frac{\sin\bar{\alpha}^2}{\cos\bar{\alpha}} + \sin\bar{\alpha} + \frac{\bar{\mu}\bar{\nu}}{\bar{\alpha}^2}\sin\bar{\alpha} + \bar{\alpha}\cos\bar{\alpha} - \frac{\bar{\mu}\bar{\mu}}{\bar{\alpha}}\cos\bar{\alpha} = 0, \tag{3.69}$$

which on simplification we get

$$\bar{\alpha}^3 + \bar{\alpha}^2\sin\bar{\alpha}\cos\bar{\alpha} = \bar{\mu}\bar{\nu}\bar{\alpha} - \bar{\mu}\bar{\nu}\sin\bar{\alpha}\cos\bar{\alpha}, \tag{3.70}$$

or

$$\bar{\mu}\bar{\nu} = \bar{\alpha}^2\left(\frac{\bar{\alpha} + \sin\bar{\alpha}\cos\bar{\alpha}}{\bar{\alpha} - \sin\bar{\alpha}\cos\bar{\alpha}}\right), \tag{3.71}$$

or

$$\bar{\mu}\bar{\nu} = \bar{\alpha}^2\left(\frac{2\bar{\alpha} + \sin 2\bar{\alpha}}{2\bar{\alpha} - \sin 2\bar{\alpha}}\right). \tag{3.72}$$

The overbar show that these are EP_2 values of the parameter. At the second exceptional point EP_2, the value α_1 is a double root of the equation $K(s) = 0$, and since the derivative $K'(s_1) = 0$ also vanishes, the coefficient P_1 becomes zero. As a result, the eigenfunction $Y_1(y)$ becomes self-orthogonal, and the systems of equations (3.49) and (3.55) become degenerate, meaning they become linearly dependent and no longer span the full solution space.

To simplify the structure of the eigenfunction expansion at the second exceptional point EP_2, rewriting the waveform in terms of y and its derivatives, rather than the original form involving s and derivatives with respect to s, simplifies the analysis and provides a more convenient representation. This done by noting (3.62) which on simplification leads to

$$Y' = \frac{\partial Y}{\partial s} = -\frac{s_1 y}{\alpha_1^2}(-\alpha_1\sin(\alpha_1 y) - \mu\cos(\alpha_1 y)) - \frac{s_1\mu\sin(\alpha_1 y)}{\alpha_1^3}, \tag{3.73}$$

or

$$Y' = \frac{\partial Y}{\partial s} = -\frac{s_1 y}{\alpha_1^2}\frac{\partial Y_1}{\partial y} - \frac{s_1\mu\sin(\alpha_1 y)}{\alpha_1^3}. \tag{3.74}$$

Now we eliminating $\sin(\alpha_1 y)$ by using (3.38), we get

$$\frac{\partial Y_1}{\partial y} = -\alpha_1 \sin(\alpha_1 y) - \mu \cos(\alpha_1 y). \tag{3.75}$$

Adding (3.38) and (3.75), we get

$$\sin \alpha_1 y = \frac{-\alpha_1}{\alpha_1^2 + \mu^2} \left(\mu Y_1 + \frac{\partial Y_1}{\partial y} \right). \tag{3.76}$$

Now using (3.76) in (3.74), we found

$$Y' = -\frac{s_1 y}{\alpha_1^2} \frac{\partial Y_1}{\partial y} \left(y - \frac{\mu}{\alpha_1^2 + \mu^2} \right) + \frac{s_1 \mu^2}{\alpha_1^2(\alpha_1^2 + \mu^2)} Y_1, \tag{3.77}$$

or

$$Y' = -\frac{s_1 y}{\alpha_1^2} \chi(y) + \frac{s_1 \mu^2}{\alpha_1^2(\alpha_1^2 + \mu^2)} Y_1, \tag{3.78}$$

where

$$\chi(y) = \left(y - \frac{\mu}{\alpha_1^2 + \mu^2} \right) \partial_y Y_1. \tag{3.79}$$

Therefore, at the point EP_2, the eigenfunction expansion for ψ_2 takes on a special form, which we will refer to as the enhanced eigenfunction expansion.

$$\psi_2 = \bar{B}_1 \left[\frac{s_1}{\alpha_1^2} \chi(y) - ixY_1(y) \right] e^{is_1 x} + \sum_{n=1}^{\infty} B_n Y_n e^{is_n x}, \tag{3.80}$$

and

$$\int_0^1 \chi(y) Y_n(y) dy = Q\delta_{1n}. \tag{3.81}$$

Additionally, it is noteworthy that the parameter Q becomes zero at the third exceptional point EP_3.

Continuity of Pressure

To check the continuity of pressure for exceptional points two use (3.28) and (3.80) in (3.45), we get

$$F+\sum_{n=0}^{\infty}A_n\cos(n\pi y)=\bar{B}_1\left(\frac{s_1}{\alpha_1^2}\chi(y)\right)+\sum_{n=1}^{\infty}B_nY_n(y). \tag{3.82}$$

Multiply (3.82) with $\cos(m\pi y)$ and integrating from 0 to 1,

$$\begin{aligned}&F\int_0^1\cos(m\pi y)dy+\sum_{n=0}^{\infty}A_n\int_0^1\cos(m\pi y)\cos(n\pi y)dy\\&=\bar{B}_1\frac{S_1}{\alpha_1^2}\int_0^1\cos(m\pi y)\chi(y)dy+\sum_{n=1}^{\infty}B_n\int_0^1\cos(m\pi y)Y_n(y)dy,\end{aligned} \tag{3.83}$$

using (3.43) and (3.50) in (3.83), we found

$$F\delta_{m0}+\sum_{n=0}^{\infty}A_n\delta_{mn}\frac{\epsilon_m}{2}=\bar{B}_1\frac{S_1}{\alpha_1^2}M_m+\sum_{n=1}^{\infty}B_nL_{mn}, \tag{3.84}$$

which contain

$$M_m=\int_0^1\cos(m\pi y)\chi(y)dy, \tag{3.85}$$

and

$$A_m=\frac{-2F\delta_{m0}}{\epsilon_m}+\frac{2s_1}{\alpha_1^2\epsilon_m}\bar{B}_1M_m+\frac{2}{\epsilon_m}\sum_{n=1}^{\infty}B_nL_{mn}. \tag{3.86}$$

Continuity of normal velocity

To check the continuity of normal velocity for exceptional points two use (3.28) and (3.80) in (3.51), we get

$$i\sum_{n=1}^{\infty}B_ns_nY_n=ikF-i\sum_{n=0}^{\infty}A_n\eta_n\cos(n\pi y). \tag{3.87}$$

Multiply(3.87) through $Y_j(y)$ and integrate 0 to 1,

$$\sum_{n=1}^{\infty}B_ns_n\int_0^1Y_nY_jdy=kF\int_0^1Y_nY_jdy-\sum_{=0}^{\infty}A_n\eta_n\int_0^1Y_j\cos(n\pi y), \tag{3.88}$$

on using orthogonality relation (3.43) and (3.50) in (3.88), we get

$$\sum_{n=1}^{\infty} B_n s_n \delta_{jn} P_j = kFL_{0j} - \sum_{n=1}^{\infty} A_n \eta_n L_{nj}, \tag{3.89}$$

which on simplification leads to

$$B_j = \frac{kFL_{0j}}{s_j P_j} - \frac{1}{s_j P_j} \sum_{n=1}^{\infty} A_n \eta_n L_{nj}, \quad j \geq 1. \tag{3.90}$$

Since $Y_1(y)$ is self orthogonal for $j \geq 1$ and have no information about B and $\bar{B}$. As a result, two additional equations emerge, one for B and another for $\bar{B}$

$$\psi_2 = \bar{B}_1 \left[\frac{s_1}{\alpha_1^2} \chi(y) - ixY_1(y) \right] e^{is_1 x} + \sum_{n=1}^{\infty} B_n Y_n e^{is_n x}. \tag{3.91}$$

On using conditions of (3.51), we get

$$\bar{B}_1 \left(\frac{s_1^2}{\alpha_1^2} \chi(y) \right) - \bar{B}_1 Y_1 + B_1 Y_1 s_1 = kF - \sum_{n=0}^{\infty} A_n \eta_n \cos(n\pi y). \tag{3.92}$$

Multiplying (3.92) with Y_1 and integrate 0 to 1, we get

$$\begin{aligned} \bar{B}_1 \frac{s_1^2}{\alpha_1^2} \int_0^1 \chi(y) Y_1 dy - \bar{B}_1 \int_0^1 Y_1^2 dy + B_1 s_1 \int_0^1 Y_1^2 dy \\ = kF \int_0^1 Y_1 dy - \sum_{n=0}^{\infty} A_n \eta_n \int_0^1 \cos(n\pi y) Y_1 dy, \end{aligned} \tag{3.93}$$

on using orthogonality relation (3.44), (3.50) and (3.81) into (3.93), we get

$$\bar{B}_1 \frac{s_1^2}{\alpha_1^2} Q = kFL_{01} - \sum_{n=0}^{\infty} A_n \eta_n L_{n1}. \tag{3.94}$$

Multiplying $\chi(y)$ with (3.92) and integrate 0 to 1, we get

$$\begin{aligned} \bar{B}_1 \frac{s_1^2}{\alpha_1^2} \int_0^1 \chi(y)^2 dy - \bar{B}_1 \int_0^1 Y_1 \chi(y) dy + B_1 s_1 \int_0^1 Y_1 \chi(y) dy \\ = kF \int_0^1 \chi(y) dy - \sum_{n=0}^{\infty} A_n \eta_n \int_0^1 \cos(n\pi y) \chi(y) dy. \end{aligned} \tag{3.95}$$

on using orthogonality relation (3.50), (3.81), and (3.85) into (3.95), we get

$$\bar{B}_1 \frac{s_1^2}{\alpha_1^2} T - \bar{B}_1 Q + B_1 s_1 Q = kFM_0 - \sum_{n=0}^{\infty} A_n \eta_n L_{mn}. \tag{3.96}$$

From (3.94) and (3.96)

$$\begin{pmatrix} s_1 Q & \frac{s_1^2}{\alpha_1^2} T - Q \\ 0 & \frac{s_1^2}{\alpha_1^2} \end{pmatrix} \begin{pmatrix} B_1 \\ \bar{B}_1 \end{pmatrix} = \begin{pmatrix} kFM_0 - \sum_{n=0}^{\infty} A_n \eta_n L_{mn} \\ kFL_{01} - \sum_{n=0}^{\infty} A_n \eta_n L_{n1} \end{pmatrix}, \tag{3.97}$$

where

$$T = \int_0^1 \chi^2(y) dy. \tag{3.98}$$

3.5 Enhanced Mode-Matching Solution with Three Exceptional Point

An EP_3 arises when their exist the possibility whereby $K = 0$, $K' = 0$ and $K'' = 0$ with respect to s. This condition leads to the existence of another wavefunction

$$\psi EP3 = \frac{\partial^2}{\partial s^2}(Y e^{isx}) = (Y'' + 2ixY' - x^2 Y)e^{isx}. \tag{3.99}$$

Now for EP_3 we put $K^{''}(s) = 0$. Taking derivative of (3.67) with respect to s, we get

$$-q\cos\bar{\bar{\alpha}} + \cos\bar{\bar{\alpha}} + \frac{p}{\bar{\bar{\alpha}}^2\cos\bar{\bar{\alpha}}} - \frac{2p}{\bar{\bar{\alpha}}^3\sin\bar{\bar{\alpha}}} + \cos\bar{\bar{\alpha}} - \bar{\bar{\alpha}}\sin\bar{\bar{\alpha}} + \frac{p}{\bar{\bar{\alpha}}\sin\bar{\bar{\alpha}}} + \frac{p}{\bar{\bar{\alpha}}^2\cos\bar{\bar{\alpha}}} = 0. \tag{3.100}$$

Now using (3.66) and (3.72) in (3.100), we get

$$(\bar{\bar{\alpha}} - \frac{\bar{\bar{\mu}}\bar{\bar{\nu}}}{\bar{\bar{\alpha}}})\cos\bar{\bar{\alpha}}\tan\bar{\bar{\alpha}} + 2\cos\bar{\bar{\alpha}} + 2\cos\bar{\bar{\alpha}}(\frac{2\bar{\bar{\alpha}} + \sin 2\bar{\bar{\alpha}}}{2\bar{\bar{\alpha}} - \sin 2\bar{\bar{\alpha}}}), \tag{3.101}$$

$$2\cos\bar{\bar{\alpha}} + 2\cos\bar{\bar{\alpha}}\frac{(2\bar{\bar{\alpha}} + \sin 2\bar{\bar{\alpha}})}{(2\bar{\bar{\alpha}} - \sin 2\bar{\bar{\alpha}})} - \frac{2\,(2\bar{\bar{\alpha}} + \sin 2\bar{\bar{\alpha}})}{\bar{\bar{\alpha}}(2\bar{\bar{\alpha}} - \sin 2\bar{\bar{\alpha}})}\sin\bar{\bar{\alpha}} = 0, \tag{3.102}$$

simplification leads to

$$8\bar{\bar{\alpha}}^2\cos\bar{\bar{\alpha}} - 4\bar{\bar{\alpha}}\sin\bar{\bar{\alpha}} - 2\sin 2\bar{\bar{\alpha}}\sin\bar{\bar{\alpha}} = 0, \tag{3.103}$$

which on simplification leads to

$$4\bar{\bar{\alpha}}^2\cos\bar{\bar{\alpha}} - 2\bar{\bar{\alpha}}\sin\bar{\bar{\alpha}} - \sin 2\bar{\bar{\alpha}}\sin\bar{\bar{\alpha}} = 0$$

$$4\cos\bar{\bar{\alpha}} - \frac{2\bar{\bar{\alpha}}\sin\bar{\bar{\alpha}}}{\bar{\bar{\alpha}}^2} - \frac{\sin 2\bar{\bar{\alpha}}\sin\bar{\bar{\alpha}}}{\bar{\bar{\alpha}}} = 0$$

$$4\cos\bar{\bar{\alpha}} - \frac{\sin\bar{\bar{\alpha}}}{\bar{\bar{\alpha}}}(2\bar{\bar{\alpha}} - \sin 2\bar{\bar{\alpha}}) = 0. \tag{3.104}$$

The wall parameters can be determined by utilizing equations (3.66) and (3.72). The double overbar shows that these are EP_3 values of the parameters. At the third exceptional point $EP3$, the value α_1 is a triple root of the equation $K(s) = 0$, meaning that the equation is satisfied not only for α_1.

But also for its first and second derivatives with respect to s. In this scenario, the eigenfunction $Y_1(y)$ is self-orthogonal, meaning that it is orthogonal to itself, and additionally, the function $\chi(y)$ is also orthogonal to $Y_1(y)$.

As a result, both the coefficients P_1 and Q vanish, indicating a higher degree of degeneracy in the system. As a consequence, the determinant of the matrix on the left-hand side of equation (3.97) vanishes, indicating that the system is degenerate.

Therefore, an additional function is necessary to represent ψ_2 as an eigenfunction expansion, and this function is related to equation (3.99). Now we partially

differentiate (3.77) with respect to s, we get

$$\begin{aligned}\left(\frac{\partial^2 Y}{\partial s^2}\right)_{s=s_1} = &-\frac{\alpha_1^2+2s_1^2}{\alpha_1^4}\left(y-\frac{\mu}{\alpha_1^2+\mu^2}\right)\frac{\partial Y_1}{\partial y}+\frac{\partial}{\partial y}\left(\frac{\partial Y_1}{\partial s_1}\right)\\ &\left(-\frac{s_1}{\alpha_1^2}y+\frac{s_1\mu}{\alpha_1^2(\alpha_1^2+\mu^2)}\right)+\frac{s_1}{\alpha_1^2}\frac{\partial Y_1}{\partial y}\left(\frac{2\mu s_1}{(\alpha_1^2+\mu^2)^2}\right)\\ &+\frac{\alpha_1^2+2s_1^2}{\alpha_1^4}\left(\frac{\mu^2}{\alpha^2+\mu^2}\right)Y_1+\frac{s_1}{\alpha_1^2}Y_1\left(\frac{2\mu^2 s_1}{(\alpha_1^2+\mu^2)^2}\right)\\ &+\frac{s_1\mu^2}{\alpha_1^2(\alpha_1^2+\mu^2)}\frac{\partial Y_1}{\partial s_1},\end{aligned} \tag{3.105}$$

some mathematical arrangement, we get

$$\begin{aligned}\left(\frac{\partial^2 Y}{\partial s^2}\right)_{s=s_1} = &-\frac{\alpha_1^2+2s_1^2}{\alpha_1^4}\chi(y)+\frac{s_1^2}{\alpha^4}\chi(y)-\frac{s_1^2}{\alpha^2}\left(y-\frac{\mu}{\alpha^2+\mu^2}\right)^2 Y_1\\ &-\frac{s_1^2\mu^2}{\alpha_1^4(\alpha_1^2+\mu^2)}\chi(y)+\frac{2s_1^2\mu}{\alpha_1^2(\alpha_1^2+\mu^2)^2}\frac{\partial Y_1}{\partial y}+\frac{\alpha_1^2+2s_1^2}{\alpha_1^4}\left(\frac{\mu^2}{\alpha^2+\mu^2}\right)Y_1\\ &+\frac{2s_1^2\mu^2}{\alpha_1^2(\alpha_1^2+\mu^2)^2}Y_1-\frac{s_1^2\mu^2}{\alpha_1^4(\alpha_1^2+\mu^2)}\chi(y)+\frac{s_1^2\mu^4}{\alpha_1^4(\alpha_1^2+\mu^2)^2}Y_1(y),\end{aligned} \tag{3.106}$$

simplification leads to

$$\begin{aligned}\left(\frac{\partial^2 Y}{\partial s^2}\right)_{s=s_1} = &-\frac{s_1^2}{\alpha_1^2}\left(\left\{(y-\frac{\mu}{\alpha^2+\mu^2}\right\}^2 Y_1-\frac{2\mu}{(\alpha_1^2+\mu^2)^2}\frac{\partial Y_1}{\partial y}\right)\\ &+\chi(y)\left(\frac{-(\alpha_1^2+\mu^2)(\alpha^2+\mu^2)-2s_1^2\mu^2}{\alpha^4}(\alpha^2+\mu^2)\right)\\ &+Y_1\left(\frac{\mu^2}{\alpha^2(\alpha^2+\mu^2)}+\frac{\mu^2 s_1^2(4\alpha^2+3\mu^2)}{\alpha^4(\alpha^2+\mu^2)^2}\right),\end{aligned} \tag{3.107}$$

simplification leads to

$$\left(\frac{\partial^2 Y}{\partial s^2}\right)_{s=s_1} = -\frac{s_1^2}{\alpha_1^2}\left(\left(y-\frac{\mu}{\alpha^2+\mu^2}\right)^2 Y_1 - \frac{2\mu}{(\alpha_1^2+\mu^2)^2}\frac{\partial Y_1}{\partial y}\right) + \chi(y)\left(\frac{2s_1^2}{\alpha_1^2(\alpha_1^2+\mu^2)} - \frac{\alpha_1^2+3s_1^2}{\alpha_1^4}\right) + Y_1\left(\frac{\mu^2}{\alpha_1^2(\alpha_1^2+\mu^2)} + \frac{\mu^2 s_1^2(4\alpha_1^2+3\mu^2)}{\alpha_1^4(\alpha_1^2+\mu^2)^2}\right), \tag{3.108}$$

$$\left(\frac{\partial^2 Y}{\partial s^2}\right)_{s=s_1} = -\frac{s_1^2}{\alpha_1^2}\xi(y) + \gamma(s_1)\chi(y) + CY_1(y), \tag{3.109}$$

where

$$\xi(y) = \left(y-\frac{\mu}{\alpha^2+\mu^2}\right)^2 Y_1 - \frac{2\mu}{(\alpha_1^2+\mu^2)^2}\partial_y Y_1, \tag{3.110}$$

and

$$\gamma(s_1) = \frac{2s_1^2}{\alpha_1^2(\alpha_1^2+\mu^2)} - \frac{\alpha_1^2+3s_1^2}{\alpha_1^4}. \tag{3.111}$$

In the EP3 scenario, C is a constant whose value doesn't depend on y, with its exact definition left undefined.:

$$\psi_2 = \bar{\bar{B}}_1\left[\frac{-s_1}{\alpha_1^2}\xi(y) + \gamma(s_1)\chi(y) - 2ix\Big\{\frac{s_1}{\alpha_1^2}\xi(y) - \frac{s_1\mu^2 Y_1(y)}{\alpha_1^2(\alpha_1^2+\mu^2)}\Big\} - x^2 Y_1(y)\right]e^{is_1x} + \bar{B}_1\left[\frac{s_1}{\alpha_1^2}\chi(y) - ixY_1(y)\right]e^{is_1x} + \sum_{n=1}^{\infty} B_n Y_n e^{is_n x}, \quad x>0 \tag{3.112}$$

where $\bar{\bar{B}}$ represents a new additional function, denoted by the double bar notation, which arises due to the triple root nature of α_1. And $\xi(y)$ has the following orthogonality property

$$\int_0^1 \xi(y)Y_n(y)dy = R\delta_{1n}. \tag{3.113}$$

Continuity of Pressure

On using (3.28) and (3.112) into (3.45), we get

$$F+\sum_{n=0}^{\infty}A_n\cos(n\pi y)=\bar{\bar{B}}_1\big[\frac{-s_1}{\alpha_1^2}\xi(y)+\gamma s_1\chi(y)-2ix\big(\frac{s_1}{\alpha_1^2}\xi(y)-\frac{s_1\mu^2Y_1(y)}{\alpha_1^2(\alpha_1^2+\mu^2)}\big)$$
$$-x^2Y_1(y)\big]e^{is_1x}+\bar{B}_1\frac{s_1}{\alpha_1^2}\chi(y)+\sum_{n=1}^{\infty}B_nY_n(y). \tag{3.114}$$

Multiply (3.114) with $\cos(m\pi y)$ and integrating from 0 to 1

$$F\int_0^1\cos(m\pi y)dy+\sum_{n=0}^{\infty}A_n\int_0^1\cos(m\pi y)\cos(n\pi y)dy$$
$$=\bar{\bar{B}}_1\frac{-s_1}{\alpha_1^2}\int_0^1\xi(y)\cos(m\pi y)dy+\int_0^1\gamma(s_1)\chi(y)\cos(m\pi y)dy$$
$$+\bar{B}_1\frac{s_1}{\alpha_1^2}\int_0^1\cos(m\pi y)\chi(y)dy+\sum_{n=1}^{\infty}B_n\int_0^1\cos(m\pi y)Y_n(y)dy, \tag{3.115}$$

or

$$F\delta_{m0}+\sum_{n=0}^{\infty}A_n\delta_{mn}\frac{\epsilon_m}{2}=\bar{\bar{B}}_1\left[\frac{-s_1^2}{\alpha_1^2}N_m+\gamma(s_1)M_m\right]+\bar{B}_1\frac{s_1}{\alpha_1^2}M_m+\sum_{n=1}^{\infty}B_nL_{mn}, \tag{3.116}$$

which leads to

$$A_m=-\frac{2}{\epsilon_m}F\delta_{m0}+\frac{2}{\epsilon_m}\bar{\bar{B}}_1\left[\frac{-s_1}{\alpha_1^2}N_m+\gamma(s_1)M_m\right]+\frac{2}{\epsilon_m}\bar{B}_1\frac{s_1}{\alpha_1^2}M_m+\frac{2}{\epsilon_m}\sum_{n=1}^{\infty}B_nL_{mn}, \tag{3.117}$$

where

$$N_m=\int_0^1\xi(y)\cos(m\pi y)dy. \tag{3.118}$$

While Continuity of Normal Velocity gives:

$$B_j = \frac{KFL_{0j}}{s_j P_j} - \frac{1}{s_j P_j}\sum_{n=1}^{\infty} A_n \eta_n L_{nj} j > 1, \tag{3.119}$$

This holds true only for values of j greater than 1. For the special case of $j = 1$, the expression takes a different form, denoted by $\bar{\bar{B}}_1$. Find out using (3.55).

Continuity of Normal Velocity

Using (3.28) and (3.112) into (3.51), we get

$$\begin{aligned}
&\bar{\bar{B}}_1\left[\frac{-s_1^3}{\alpha_1^2}\xi(y) + \gamma(s_1)\chi(y)s_1 - 2\left(\frac{s_1}{\alpha_1^2}\xi(y) - \frac{s_1\mu^2 Y_1(y)}{\alpha_1^2(\alpha_1^2+\mu^2)}\right)\right] \\
&+ \bar{B}_1\left[\frac{s_1^2}{\alpha_1^2}\chi(y) - Y_1(y)\right] + \sum_{n=1}^{\infty} B_n Y_n s_n = kF + \sum_{n=0}^{\infty}\eta_n A_n \cos(n\pi y).
\end{aligned} \tag{3.120}$$

Multiply (3.120) by Y_1 and integrate from 0 to 1

$$\begin{aligned}
&\bar{\bar{B}}_1\left[\int_0^1 Y_1\frac{-s_1^3}{\alpha_1^2}\xi(y)dy + s_1\gamma(s_1)\int_0^1 Y_1\chi(y)dy - 2\frac{s_1}{\alpha_1^2}\int_0^1 Y_1\xi(y)dy\right] \\
&- 2\bar{\bar{B}}_1\left[\frac{s_1\mu^2 Y_1(y)}{\alpha_1^2(\alpha_1^2+\mu^2)}\int_0^1 Y_1^2\right] \\
&+ \bar{B}_1\left[\frac{s_1^2}{\alpha_1^2}\int_0^1 Y_1\chi(y)dy - \int_0^1 Y_1^2(y)\right] \\
&+ \sum_{n=1}^{\infty} B_n\int_0^1 Y_1^2 s_n = kF\int_0^1 Y_1 + \sum_{n=0}^{\infty}\eta_n A_n\int_0^1 Y_1\cos(n\pi y)dy,
\end{aligned} \tag{3.121}$$

which leads to

$$\bar{\bar{B}}_1\frac{-s_1^3}{\alpha_1^2}R = kFL_{01} + \sum_{n=0}^{\infty}\eta_n A_n L_{mn}. \tag{3.122}$$

Multiply (3.120) by $\chi(y)$ and integrate 0 to 1

$$\bar{\bar{B}}_1\left[\frac{-s_1^3}{\alpha_1^2}\int_0^1\chi(y)\xi(y)dy+s_1\gamma(s_1)\int_0^1\chi^2(y)dy\right]-2\bar{\bar{B}}_1\frac{s_1}{\alpha_1^2}\int_0^1\chi^2(y)dy$$
$$-2\bar{\bar{B}}_1\frac{s_1\mu^2}{\alpha_1^2(\alpha_1^2+\mu^2)}\int_0^1\chi(y)Y_1dy+\bar{B}_1\left[\frac{s_1^2}{\alpha_1^2}\int_0^1\chi^2(y)dy-\int_0^1\chi(y)Y_1(y)dy\right]$$
$$+\sum_{n=1}^{\infty}B_ns_n\int_0^1\chi(y)Y_ndy=kF\int_0^1\chi(y)dy+\sum_{n=0}^{\infty}\eta_nA_n\int_0^1\chi(y)\cos(n\pi y)dy, \tag{3.123}$$

some simplification leads to

$$\bar{\bar{B}}_1\left[\frac{-s_1^3}{\alpha_1^2}U+s_1\gamma(s_1)T-2\frac{s_1}{\alpha_1^2}T\right]+\bar{B}_1\frac{s_1^2}{\alpha_1^2}T=kFM_0+\sum_{n=0}^{\infty}\eta_nA_nmn \tag{3.124}$$

$$\bar{\bar{B}}_1\Omega+\bar{B}_1\frac{s_1^2}{\alpha_1^2}T=kFM_0+\sum_{n=0}^{\infty}\eta_nA_nM_n. \tag{3.125}$$

Multiply (3.120) by $\xi(y)$ and integrate 0 to 1

$$\bar{\bar{B}}_1\frac{-s_1^3}{\alpha_1^2}\int_0^1\xi^2(y)dy+\bar{\bar{B}}_1s_1\gamma(s_1)\int_0^1\chi(y)\xi(y)dy-2\bar{\bar{B}}_1\frac{s_1}{\alpha_1^2}\int_0^1\chi(y)\xi(y)dy$$
$$-2\bar{\bar{B}}_1\frac{s_1\mu^2}{\alpha_1^2(\alpha_1^2+\mu^2)}\int_0^1\xi(y)Y_1dy+\bar{B}_1\left[\frac{s_1^2}{\alpha_1^2}\int_0^1\chi(y)\xi(y)dy-\int_0^1\xi(y)Y_1(y)dy\right]$$
$$+\sum_{n=1}^{\infty}B_ns_n\int_0^1\xi(y)Y_ndy=kF\int_0^1\xi(y)dy+\sum_{n=0}^{\infty}\eta_nA_n\int_0^1\xi(y)\cos(n\pi y)dy, \tag{3.126}$$

which on simplification we get

$$\bar{\bar{B}}_1\left[\frac{-s_1^3}{\alpha_1^2}W+s_1\gamma(s_1)U-2\frac{s_1}{\alpha_1^2}U+\frac{2s_1\mu^2}{\alpha_1^2(\alpha_1^2+\mu^2)}R\right]+\bar{B}_1\frac{s_1^2}{\alpha_1^2}U-\bar{B}_1R+B_1s_1R$$
$$=kFN_0+\sum_{n=0}^{\infty}\eta_nA_nN_n, \tag{3.127}$$

or

$$\bar{\bar{B}}_1\Theta + \bar{B}_1\left(\frac{s_1^2}{\alpha_1^2}U - R\right) + B_1 s_1 R = kFN_0 + \sum_{n=0}^{\infty}\eta_n A_n N_n. \tag{3.128}$$

Now combining (3.122),(3.125) and (3.128), we get

$$\begin{pmatrix} s_1R & \frac{s_1^2}{\alpha_1^2}U - R & \Theta \\ 0 & \frac{s_1^2}{\alpha_1^2}T & \Omega \\ 0 & 0 & -\frac{s_1^3}{\alpha_1^2}R \end{pmatrix}\begin{pmatrix} B_1 \\ \bar{B}_1 \\ \bar{\bar{B}}_1 \end{pmatrix} = \begin{pmatrix} kFN_0 - \sum_{n=0}^{\infty} A_n\eta_n N_n \\ kFM_0 - \sum_{n=0}^{\infty} A_n\eta_n M_n \\ kFL_{01} - \sum_{n=0}^{\infty} A_n\eta_n L_n 1 \end{pmatrix}, \tag{3.129}$$

where

$$\Theta = \left[\frac{-s_1^3}{\alpha_1^2}W + s_1\gamma(s_1)U - 2\frac{s_1}{\alpha_1^2}U + \frac{2s_1\mu^2}{\alpha_1^2(\alpha_1^2+\mu^2)}R\right], \tag{3.130}$$

and

$$\Omega = \left[\frac{-s_1^3}{\alpha_1^2}U + s_1\gamma(s_1)T - 2\frac{s_1}{\alpha_1^2}T\right], \tag{3.131}$$

with

$$U = \int_0^1 \xi(y)\chi(y)dy \quad \text{and} \quad W = \int_0^1 \xi^2 dy. \tag{3.132}$$

The coefficients A_n $(n = 0, 1, 2, \ldots)$, $\bar{B}_1$, $\bar{\bar{B}}_1$, and B_n $(n = 1, 2, 3, \ldots)$ are determined by using equations (3.117) and (3.119), and then solving the resulting set of algebraic equations numerically, along with equation (3.129).

3.6 Numerical Results

The numerical results demonstrate a high degree of accuracy and consistency across the different regions of the fluid, confirming the effectiveness of the truncated solution approach in capturing the physical behavior of the system. The graphs show a very good match between the predicted pressures and velocities in the

fluid areas. This means that the simplified solution is accurate and effectively combines the different regions together. The excellent match confirms that the numerical method is reliable and produces trustworthy results. Here we truncate the system by taking m=n=0,1,2,...,N and the numerical calculations are carried out using the software MATHEMATICA, where the relevant parameters are set to specific values. By solving these equations, we obtain the coefficients An, B_n, $n = 0, 1, 2, \cdots, N$.

Once these scattered coefficients are known the pressures and velocities can be plotted at interface. To display the graphs, we fixed the height of the ducts at $h_1 = 0.25m$ and $h_2 = 0.35m$, $c = 343.5m/s$ and $a = 1$. The graphs illustrate the variation in pressure and velocity components as a function of duct height, normalized to a reference point at the interface where the ducts connect in figures 3.2-3.5. The physical parameters from figure 3.2-3.5 are $f = 100$, $\mu = -i$, $\nu = -i + 0.5$ and $N = 30$ terms. While from figure 3.6 to 3.9 the physical parameters are $f = 25$, $\mu = -i$, $\nu = 1 - i$ and $N = 40$ terms .

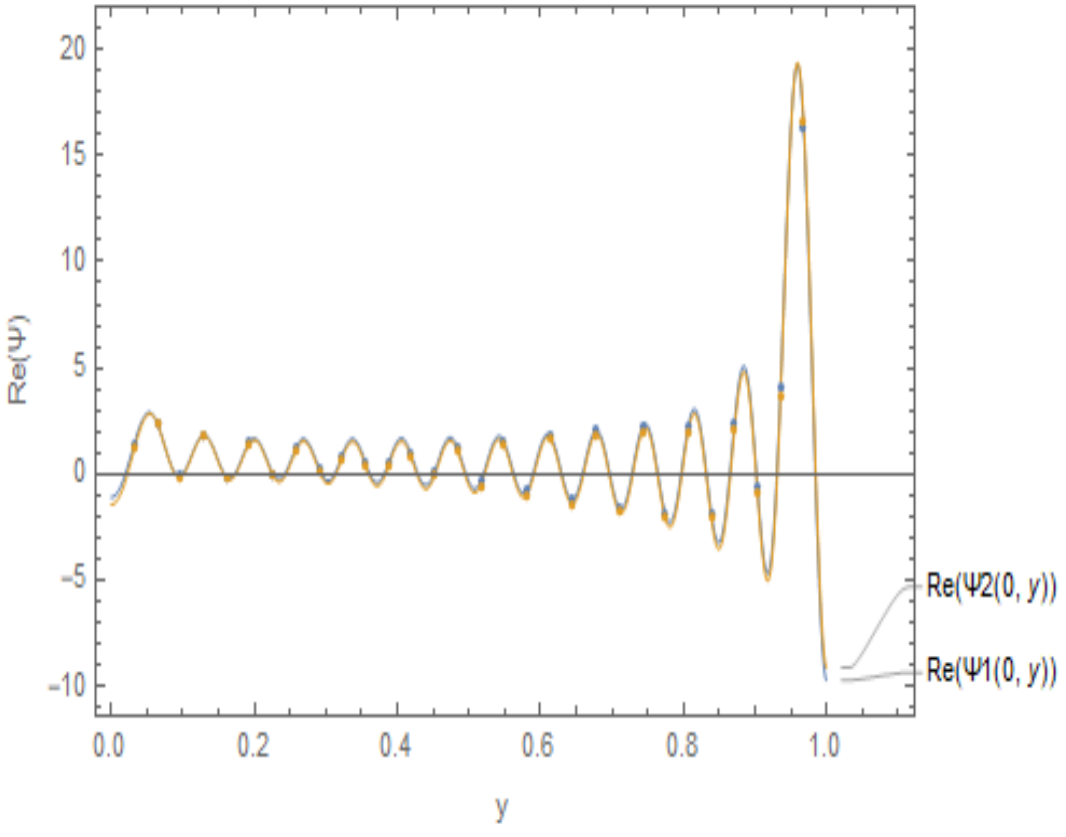

FIGURE 3.2: Real part of pressures $\psi_1(0, y)$ and $\psi_2(0, y)$.

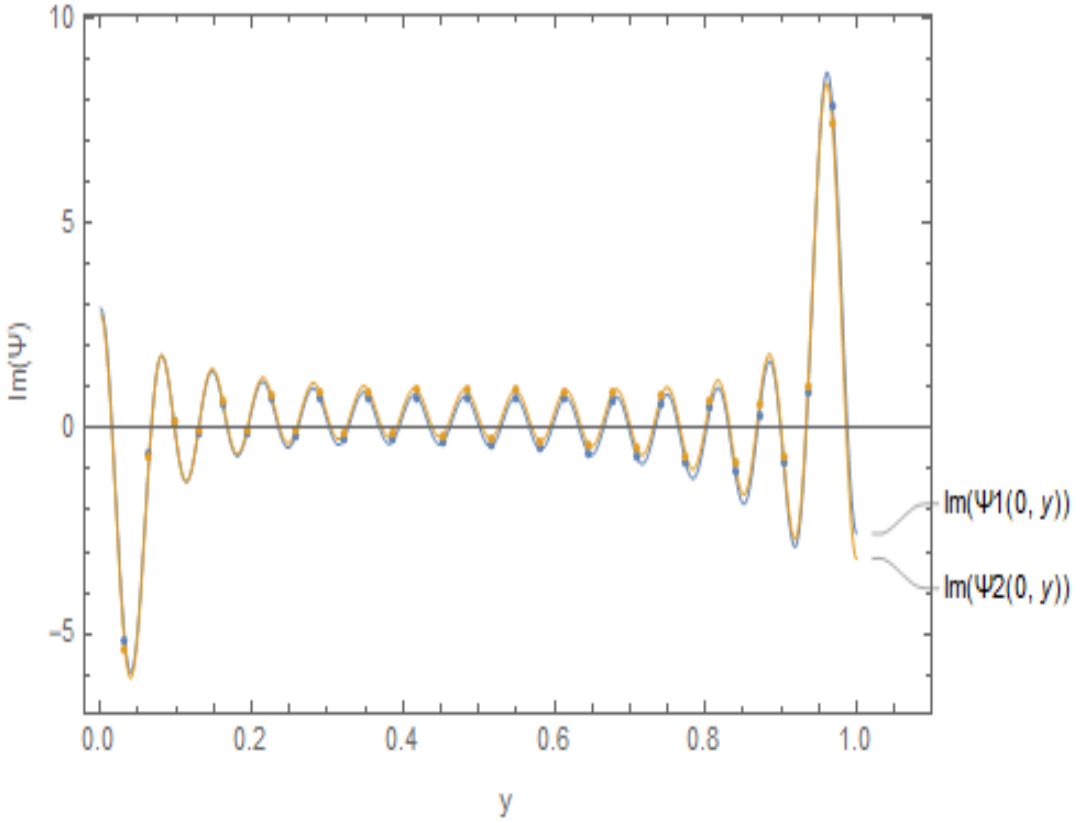

FIGURE 3.3: Imaginary part of pressures $\psi_1(0, y)$ and $\psi_2(0, y)$.

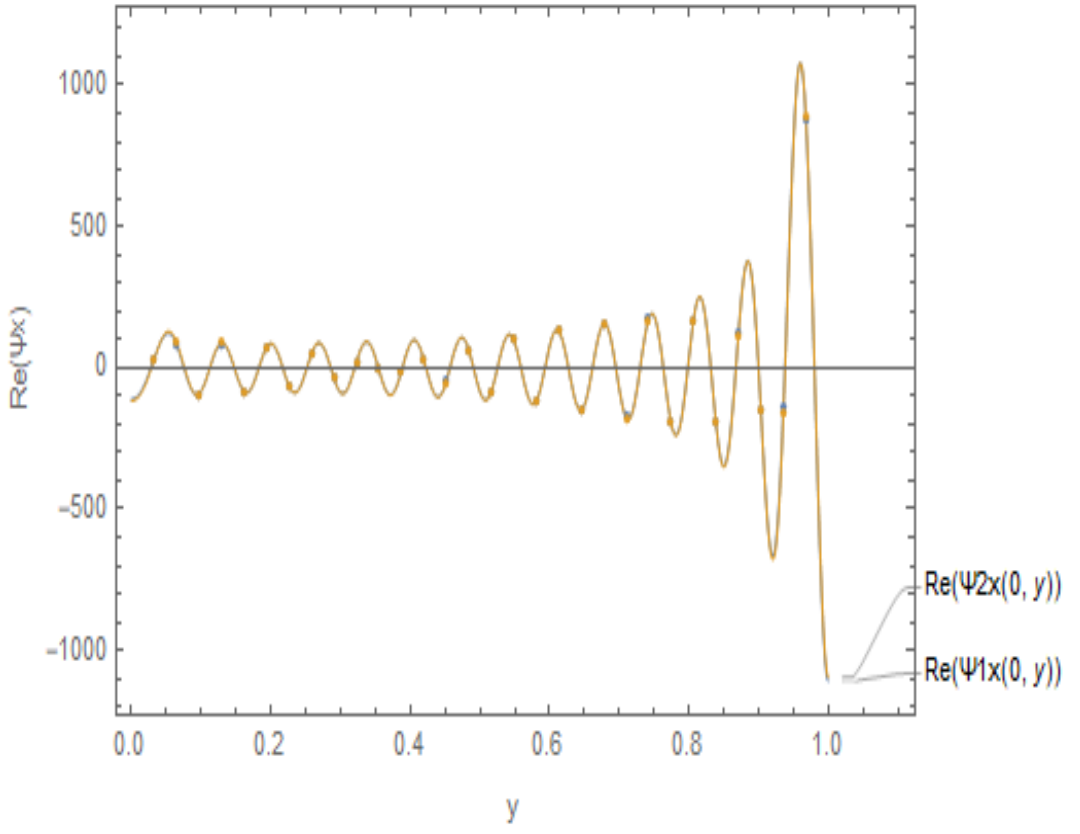

FIGURE 3.4: Real part of velocities $\psi_{1x}(0, y)$ and $\psi_{2x}(0, y)$.

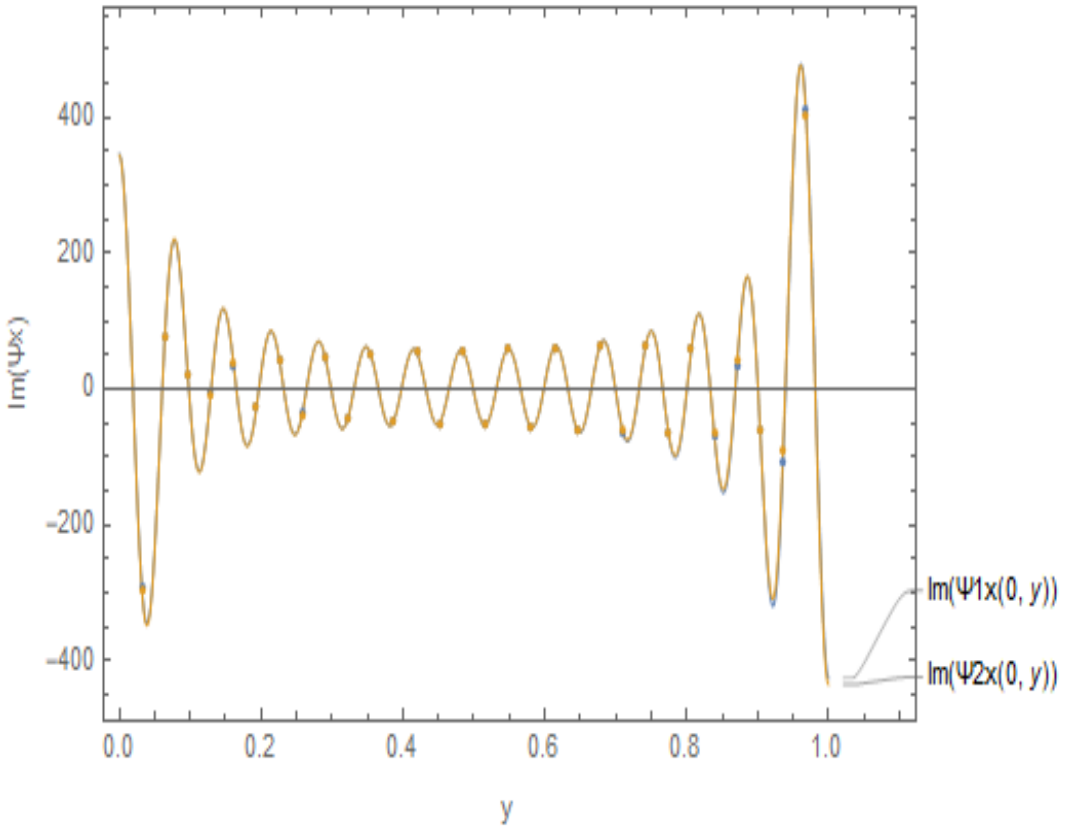

FIGURE 3.5: Imaginary part of velocities $\psi_{1x}(0, y)$ and $\psi_{2x}(0, y)$.

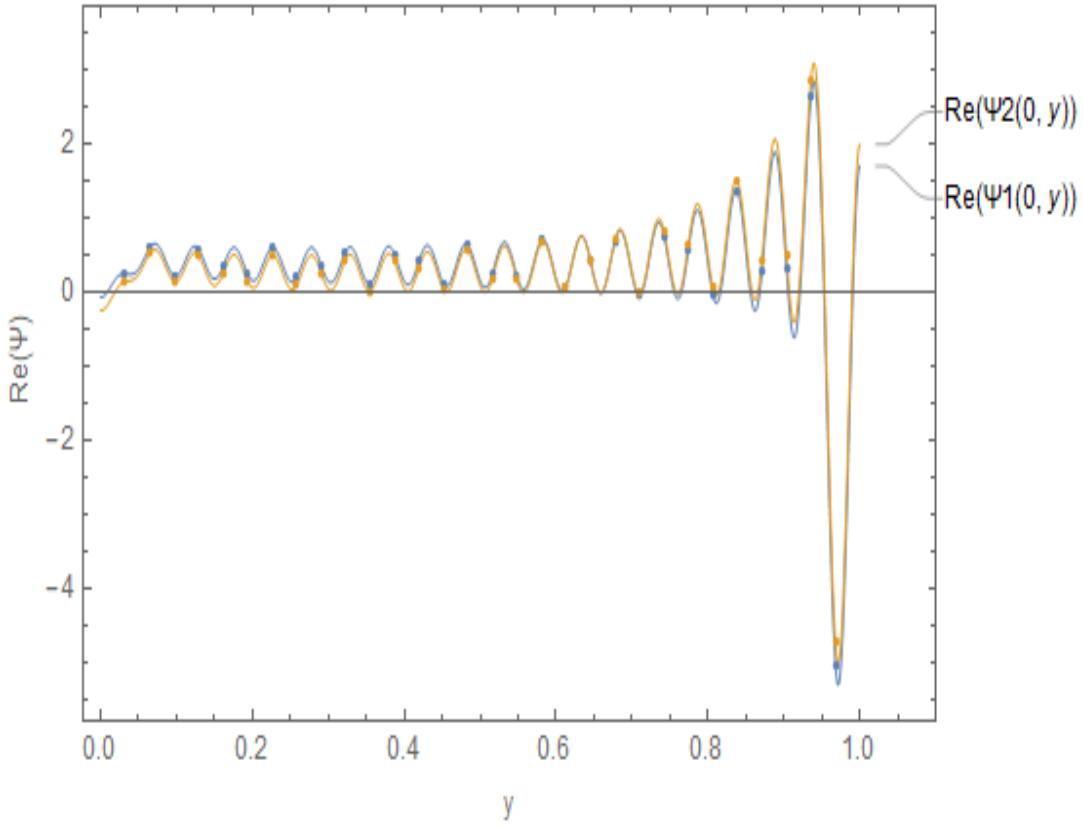

FIGURE 3.6: Real part of pressures $\psi_1(0, y)$ and $\psi_2(0, y)$.

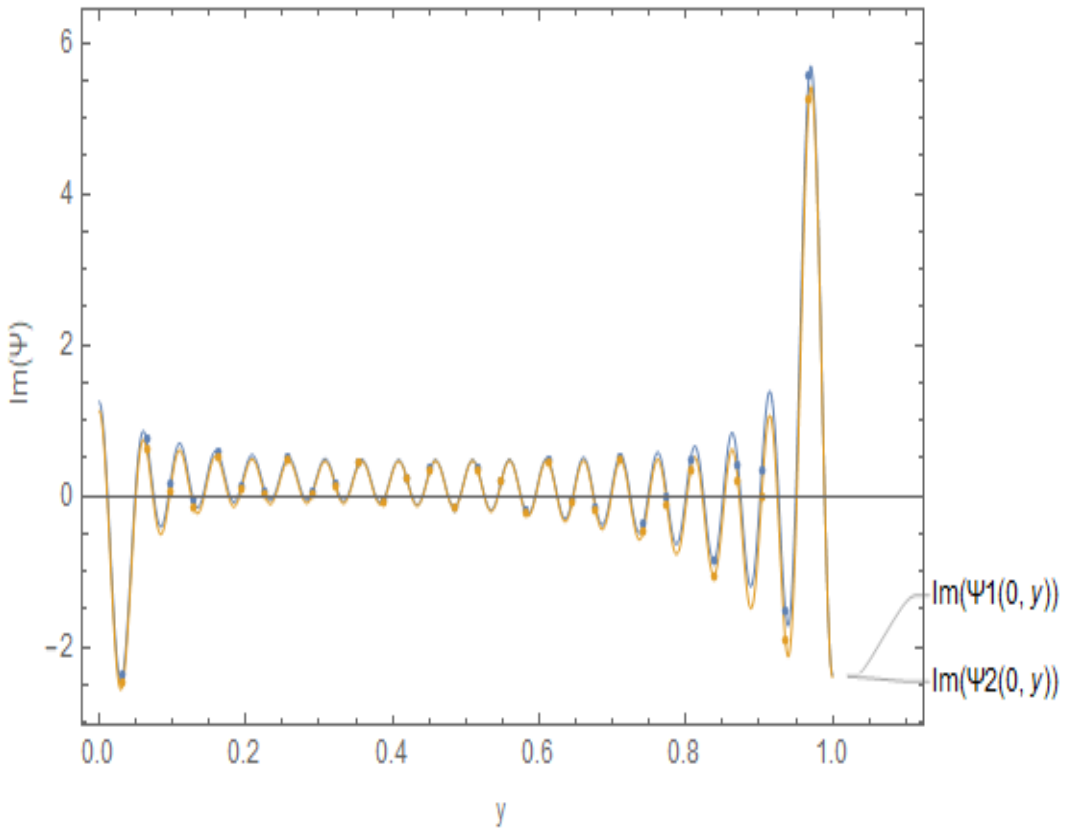

FIGURE 3.7: Imaginary part of pressures $\psi_1(0, y)$ and $\psi_2(0, y)$.

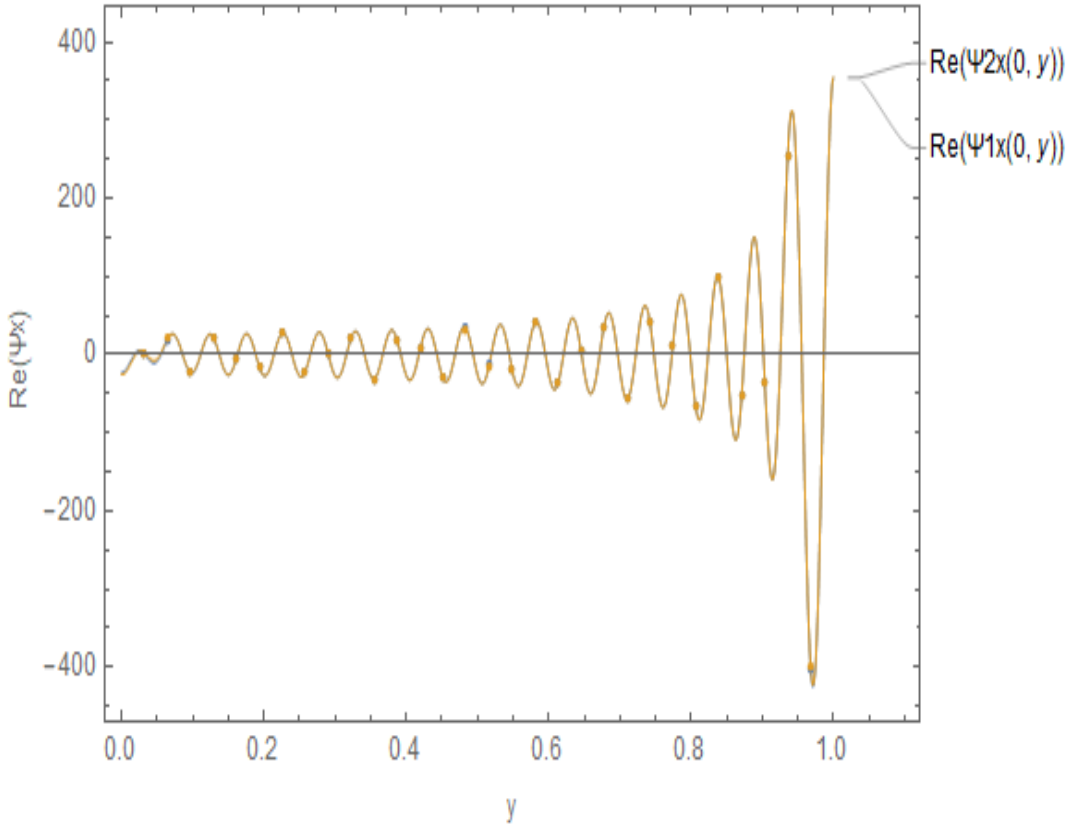

FIGURE 3.8: Real part of velocities $\psi_{1x}(0, y)$ and $\psi_{2x}(0, y)$.

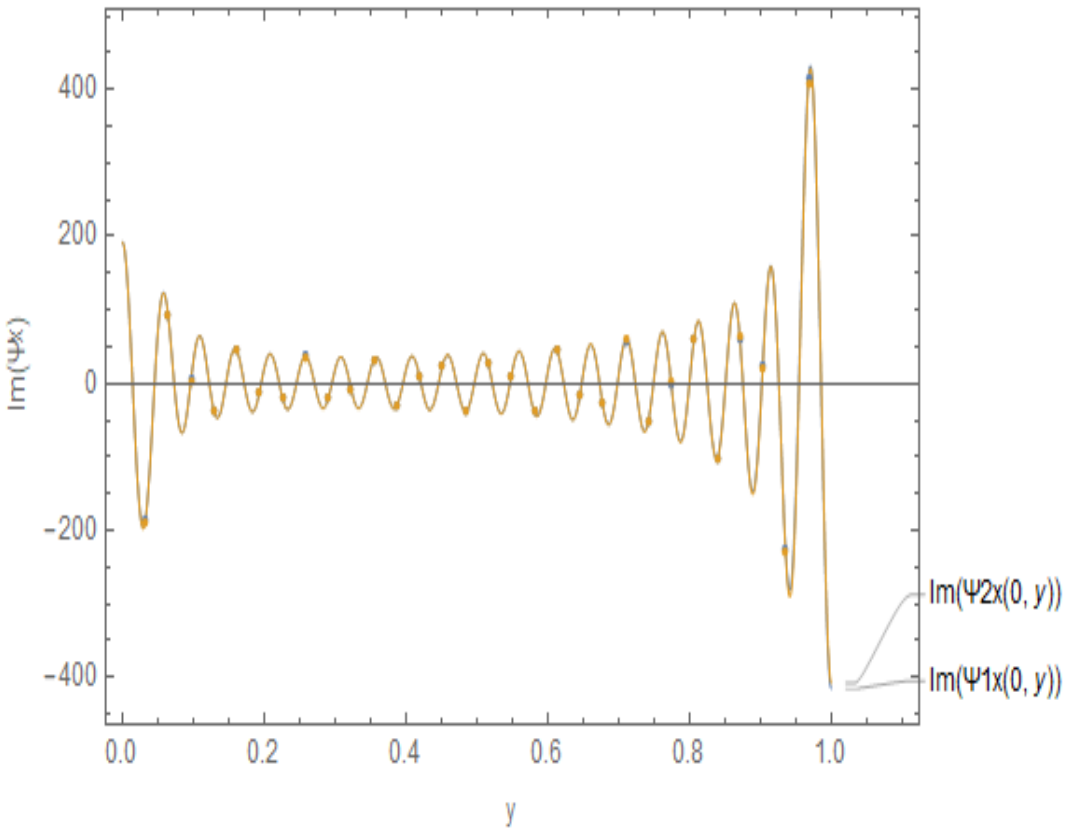

FIGURE 3.9: Imaginary part of velocities $\psi_{1x}(0, y)$ and $\psi_{2x}(0, y)$.

Figs. 3.2, 3.3 and 3.6, 3.7 show the real and imaginary parts of pressure $\psi_1(0, y)$ and $\psi_2(0, y)$ in the regions $0 \leq y \leq h_1$ and $0 \leq y \leq h_2$, respectively. The real and imaginary parts of normal velocities $\psi_{1x}(0, y)$ and $\psi_{2x}(0, y)$ for the respective regions are plotted in Figs. 3.4, 3.5 and 3.8, 3.9. The graphs show a very good match between the predicted pressures and velocities in the fluid areas. This means that the simplified solution is accurate and effectively combines the different regions together. The excellent match confirms that the numerical method is reliable and produces trustworthy results.

Chapter 4

Plane Wave Propagation with Embedded Lining Conditions in a Rigid Duct

In this chapter we examines the propagation of waves through modes in a waveguide with an embedded wire mesh. The insertion of a wire mesh parallel to the waveguides walls is a effective approach for optimizing modal attenuation. By strategically placing the wire mesh at a critical location, it is possible to achieve Exceptional Points EP_s for the first two higher order modes, leading to enhanced modal attenuation and control over wave propagation. Also consider a method for optimally filtering all modes except the plane mode in a two dimensional duct for two semi infinite sections, with a longitudinal resisting screen. We find an exceptional point where mode 1 and mode 2 merge. Then, we use mode matching scheme to find the optimal parameters of the screen since the mode 1 and 2 are optimally absorbed at the exceptional point while mode 0 is unaffected by the wire mesh.

We illustrate ability of this system to filter an acoustic field over two configurations. This chapter is arranged as fellows: The mathematical formulation and mode-matching solution are given in Sections 4.1 and 4.2. Standard mode-matching solution with no exceptional point is discussed in Section 4.3 and enhanced mode-matching solution with two exceptional points is given in Section 4.4.

4.1 Problem Formulation

These are dimensionless quantities, all lengths being in unit of the height of the waveguide a. In the waveguide, the acoustic pressure field obeys the wave equation Consider the propagation of sound waves in Fig.4.1 in the harmonic system with the convention $e^{i\omega t}$.

These are dimensionless quantities, in which all lengths being in unit of the height of the waveguide a.

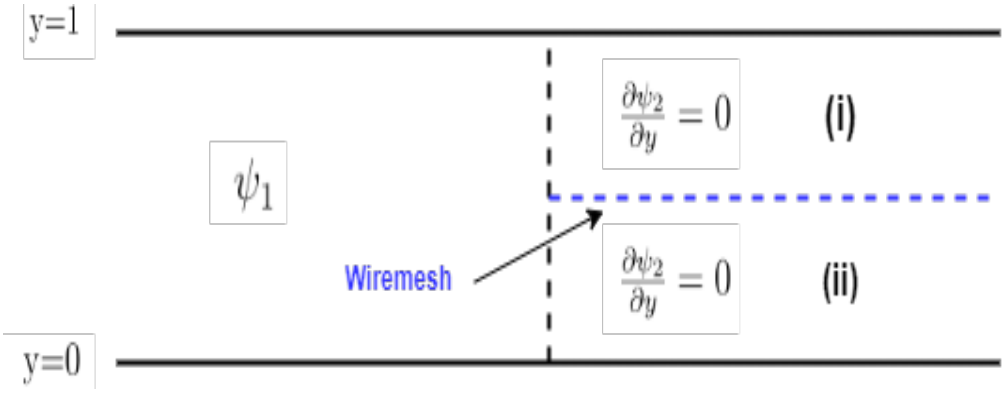

FIGURE 4.1: An infinite planar waveguide with the inserted wiremesh (blue dotted line)

In the waveguide, the acoustic pressure field obeys the wave equation

$$\left\{\frac{\partial^2}{\partial x^2} + \frac{\partial^2}{\partial y^2} + k^2\right\}\psi = 0, \tag{4.1}$$

where

$$k = \hat{k}a = \frac{w}{c}a.$$

and $\psi(x, y)$ is the dimensionless reduced fluid velocity. The duct exist in the region I and II have the following boundary conditions at $y = 0, 1$

$$\frac{\partial \psi_1}{\partial y} = 0, \tag{4.2}$$

and

$$\frac{\partial \psi_2}{\partial y} = 0. \tag{4.3}$$

As shown in Fig. 4.1 At the wire mesh located at $y = d$ we have ψ_2 as follows

$$i\frac{R}{K}\frac{\partial \psi_2}{\partial y} = [\psi_2]_{d^-}^{d^+}, \tag{4.4}$$

with R the dimensionless resistance of the wire mesh

$$iC\frac{\partial \psi_2}{\partial y} = \psi_2(d^+) - \psi_2(d^-), \tag{4.5}$$

and

$$\frac{\partial \psi_2(d^-)}{\partial y} = \frac{\partial \psi_2(d^+)}{\partial y}. \tag{4.6}$$

4.2 Solution Methodology

The mode-matching technique can be used to solve the boundary value problem which are defined in (4.1) to (4.6). Exceptional points exist here due to the involvement of lined boundary conditions. So for the solution procedure there will exist standard and enhanced mode-matching formulation. For the problem two solutions are possible.

- Standard mode-matching solution
- Enhanced mode-matching solution with two exceptional points

these solutions are explained in next sections.

4.3 Standard Mode-Matching Solution

For the standard mode-matching solution no exceptional point is involved. We determine eigenfunction expansion by using separation of variable method.

- For region $x < 0$, the governing equation (4.1) and the rigid boundary conditions (4.2) are used. By using separation of variable method this one is completely explained in previous chapter 3. Which gives us the solution

$$\psi_1 = F\cos(\pi y)e^{(i\eta_1 x)} + \sum_{n=0}^{\infty} A_n \cos(n\pi y)e^{(-i\eta_n x)}. \tag{4.7}$$

Where $\eta_n = \sqrt{k^2 - n\pi^2}$, $n = 0, 1, 2, \cdots$ and $F = \sqrt{\frac{2}{\pi}}$ which is chosen to made the incident power to unity.

- For region $x > 0$, we have governing equation (4.1) and boundary conditions (4.3) to (4.6) are involved.

As classically, we look for solutions of the Helmholtz equation in transverse mode

$$\psi_2 = Y(s, y)e^{isx}. \tag{4.8}$$

Now using (4.8) into (4.3) for region I and II at $y = 0$ and $y = 1$ respectively

$$\frac{\partial Y_1(0)}{\partial y} = 0, \tag{4.9}$$

and

$$\frac{\partial Y_2(1)}{\partial y} = 0. \tag{4.10}$$

For Region 1:

Using (4.8) into (4.1), we found

$$\frac{\partial^2 Y_1}{\partial y^2} + \alpha^2 Y_1 = 0, \tag{4.11}$$

where

$$\alpha = \sqrt{k^2 - s^2}. \tag{4.12}$$

Now solving (4.11), we get

$$Y_1 = c_1\cos(\alpha y) + c_2\sin(\alpha y), \tag{4.13}$$

using (4.9) into (4.13), we get

$$Y_1 = c_1 \cos(\alpha y), \quad \text{with} \quad c_2 = 0, \tag{4.14}$$

For Region 2:

Using (4.8) into (4.1), we found

$$\frac{\partial^2 Y_2}{\partial y^2} + \alpha^2 Y_2 = 0. \tag{4.15}$$

Now solving (4.14), we get

$$Y_2 = c_3 \cos(\alpha y) + c_4 \sin(\alpha y), \tag{4.16}$$

using (4.10) into (4.13), we get

$$Y_2 = c_4 \left\{ \frac{\cos \alpha(y-1)}{\sin \alpha} \right\}, \quad \text{with} \quad c_3 = c_4 \frac{\cos(\alpha)}{\sin(\alpha)}. \tag{4.17}$$

Now using equation (4.6) for $y = d$, we have

$$Y_1'(d) = Y_2'(d). \tag{4.18}$$

On using (4.14) and (4.17) into (4.18), we found

$$-c_1 \alpha \sin(\alpha d) = -c_4 \frac{\alpha \sin \alpha(d-1)}{\sin \alpha}, \tag{4.19}$$

simplifying (4.19), then use it in (4.17), we get

$$Y_2 = c_1 \frac{\sin(\alpha d)}{\sin \alpha(d-1)} \cos \alpha(y-1), \tag{4.20}$$

where

$$c_4 = c_1 \frac{\sin \alpha \sin(\alpha d)}{\sin \alpha(d-1)}.$$

Now using equation (4.5) for $y = d$, we have

$$iC\frac{\partial Y_1(d)}{\partial y} = Y_2(d) - Y_1(d), \tag{4.21}$$

On using (4.14) and (4.17) into (4.21), we found

$$-ic_1C\alpha\sin(\alpha d) = c_1\frac{\sin(\alpha d)}{\sin\alpha(d-1)}\cos\alpha(d-1) - c_1\cos(\alpha d), \tag{4.22}$$

which on simplification, we get

$$c_1[\sin\alpha + iC\alpha\sin(\alpha d)\sin\alpha(d-1)] = 0. \tag{4.23}$$

For non-trivial solution $c_1 \neq 0$, we have

$$D = K(s) = \sin\alpha + iC\alpha\sin(\alpha d)\sin\alpha(d-1), \tag{4.24}$$

and

$$Y(s,y) = \begin{cases} Y_1 = \cos(\alpha y) & o < y < d \\ Y_2 = \dfrac{\sin(\alpha d)}{\sin\alpha(d-1)}\cos\alpha(y-1) & d < y < 1. \end{cases} \tag{4.25}$$

here $\alpha = \sqrt{k^2 - s^2}$ are the roots of (4.25) and can be found numerically. As there can be infinite many values of α, for which (4.25) holds then the eigenfunction expansion can be given as:

$$\psi_2 = \sum_{n=1}^{\infty} B_nY_n(y)e^{(is_nx)} + \sum_{n=1}^{\infty} C_nY_n(y)e^{(-is_nx)}. \tag{4.26}$$

As there is no neglection in region at $x \geq 0$, thus $c_n = 0$ and (4.26) takes formulation

$$\psi_2 = \sum_{n=0}^{\infty} B_nY_n(y)e^{(is_nx)} \tag{4.27}$$

where B_n is the complex amplitude of nth transmitted mode and $s_n = \sqrt{1-\alpha_n^2}$, $n = 0, 1, 2, \cdots$. The eigenfunctions satisfy the following orthogonality relation

$$\int_0^d Y_{1m}(y)Y_{1n}(y)dy + \int_d^1 Y_{2m}(y)Y_{2n}(y)dy = \delta_{mn}E_n, \tag{4.28}$$

where

$$P_n = \int_0^d Y_{1n}^2(y)dy + \int_d^1 Y_{1n}^2(y)dy. \tag{4.29}$$

Note: Orthogonality of eigenfunctions from 0 to d and d to 1,

$$\frac{\partial^2 Y_{1n}}{\partial y^2} + \alpha_n^2 Y_{1n} = 0, \tag{4.30}$$

$$\frac{\partial^2 Y_{2n}}{\partial y^2} + \alpha_n^2 Y_{2n} = 0, \tag{4.31}$$

having boundary conditions:

$$\frac{dY_{1n}}{dy} = 0 \quad \text{at} \quad y = 0, \tag{4.32}$$

$$\frac{dY_{2n}}{dy} = 0 \quad \text{at} \quad y = 1, \tag{4.33}$$

$$\frac{dY_{1n}(d)}{dy} = \frac{dY_{2n}(d)}{dy}, \tag{4.34}$$

$$\frac{iR}{K}\frac{dY_{2n}}{dy} = Y_{2n}(d) - Y_{1n}(d). \tag{4.35}$$

Multiply (4.30) with Y_{1m} and integrate from 0 to d

$$\int_0^d \frac{d^2 Y_{1n}}{dy^2} Y_{1m} dy + \alpha_n^2 \int_0^d Y_{1n}Y_{1m} = 0, \tag{4.36}$$

which on simplification leads to

$$\frac{dY_{1n}}{dy} Y_{1m}|_0^d - \int_0^d \frac{d^2 Y_{1n}}{dy^2}\frac{d^2 Y_{1m}}{dy^2} dy + \alpha_n^2 \int_0^d Y_{1n}Y_{1m} = 0, \tag{4.37}$$

which leads to

$$\frac{dY_{1n}(d)}{dy}Y_{1m}(d)-\frac{dY_{1n}(0)}{dy}Y_{1m}(0)-Y_{1n}\frac{dY_{1m}}{dy}|_0^d+\int_0^d Y_{1n}\frac{d^2Y_{1m}}{dy^2}dy+\alpha_n^2\int_0^d Y_{1n}Y_{1m}=0, \tag{4.38}$$

using (4.30) into (4.38), we get

$$(\alpha_n^2-\alpha_m^2)\int_0^d Y_{1n}Y_{1m}dy=Y_{1n}(d)\frac{dY_{1m}(d)}{dy}-Y_{1m}(d)\frac{dY_{1n}(d)}{dy}. \tag{4.39}$$

Now multiply (4.31) with $Y_{2m}(y)$ and integrate d to 1

$$\int_d^1 \frac{d^2Y_{2n}}{dy^2}Y_{2m}dy+\alpha_n^2\int_d^1 Y_{2n}Y_{2m}=0, \tag{4.40}$$

which on simplification leads to

$$\frac{dY_{2n}}{dy}Y_{2m}|_d^1-\int_d^1\frac{d^2Y_{2n}}{dy^2}\frac{d^2Y_{2m}}{dy^2}dy+\alpha_n^2\int_d^1 Y_{2n}Y_{2m}=0, \tag{4.41}$$

or

$$\frac{dY_{2n}(1)}{dy}Y_{2m}(1)-\frac{dY_{2n}(d)}{dy}Y_{2m}(d)-Y_{2n}\frac{dY_{2m}}{dy}|_d^1+\int_d^1 Y_{2n}\frac{d^2Y_{2m}}{dy^2}dy+\alpha_n^2\int_d^1 Y_{2n}Y_{2m}=0, \tag{4.42}$$

using (4.30) into (4.42), we get

$$-\frac{dY_{2n}(d)}{dy}Y_{2m}(d)+Y_{2n}(d)\frac{dY_{2m}(d)}{dy}-\alpha_m^2\int_d^1 Y_{2n}Y_{2m}dy+\alpha_n^2\int_d^1 Y_{2n}Y_{2m}dy=0, \tag{4.43}$$

simplification leads to

$$(\alpha_n^2-\alpha_m^2)\int_d^1 Y_{2n}Y_{2m}dy=-Y_{2n}(d)\frac{dY_{2m}(d)}{dy}+Y_{2m}(d)\frac{dY_{2n}(d)}{dy}. \tag{4.44}$$

Now adding (4.39) and (4.44), we get

$$(\alpha_n^2 - \alpha_m^2)\left[\int_0^d Y_{1n}Y_{1m}dy + \int_d^1 Y_{2n}Y_{2m}dy\right] = Y_{1n}(d)\frac{dY_{1m}(d)}{dy} - Y_{1m}(d)\frac{dY_{1n}(d)}{dy} - Y_{2n}(d)\frac{dY_{2m}(d)}{dy} + Y_{2m}(d)\frac{dY_{2n}(d)}{dy}, \tag{4.45}$$

simplification leads to

$$(\alpha_n^2 - \alpha_m^2)\left[\int_0^d Y_{1n}Y_{1m}dy + \int_d^1 Y_{2n}Y_{2m}dy\right] = \frac{dY_{1n}(d)}{dy}[Y_{2m}(d) - Y_{1m}(d)] + \frac{dY_{1m}(d)}{dy}[Y_{1n}(d) - Y_{2n}(d)]. \tag{4.46}$$

Using (4.35) in (4.46), we have

$$(\alpha_n^2 - \alpha_m^2)\left[\int_0^d Y_{1n}Y_{1m}dy + \int_d^1 Y_{2n}Y_{2m}dy\right] = \frac{iR}{K}\frac{dY_{1n}}{dy}\frac{dY_{1m}}{dy} - \frac{iR}{K}\frac{dY_{1n}}{dy}\frac{dY_{1m}}{dy}, \tag{4.47}$$

which on simplification leads to

$$(\alpha_n^2 - \alpha_m^2)\left[\int_0^d Y_{1n}Y_{1m}dy + \int_d^1 Y_{2n}Y_{2m}dy\right] = 0, \tag{4.48}$$

where

$$\alpha_n = \alpha_m,$$

and

$$P_n = \int_0^d Y_{1n}^2(y)dy + \int_d^1 Y_{2n}^2(y)dy.$$

Now we check continuity conditions at $x = 0$, we have

Continuity of Pressure

$$\psi_1(0, y) = \psi_2(0, y), \quad 0 < y < 1, \tag{4.49}$$

using (4.7) and (4.27), we get

$$F\cos(\pi y)+\sum_{n=0}^{\infty}A_n\cos(n\pi y)=\sum_{n=1}^{\infty}B_nY_n(y). \tag{4.50}$$

Multiply (4.50) with $\cos(m\pi y)$ and integrating from 0 to d and d to 1, we get

$$\begin{aligned}&F\Big[\int_0^d\cos(\pi y)\cos(m\pi y)dy+\int_d^1\cos(\pi y)\cos(m\pi y)dy\Big]\\&+\sum_{n=0}^{\infty}A_n\Big[\int_0^d\cos(m\pi y)\cos(n\pi y)dy+\int_d^1\cos(m\pi y)\cos(n\pi y)dy\Big]\\&=\sum_{n=1}^{\infty}B_n\int_0^d\cos(m\pi y)Y_{1n}(y)dy+\int_d^1\cos(m\pi y)Y_{2n}(y)dy.\end{aligned} \tag{4.51}$$

On using orthogonality relation (4.28) and (4.29), we get

$$F\delta_{m1}\frac{\epsilon_m}{2}+\sum_{n=0}^{\infty}A_n\delta_{mn}\frac{\epsilon_m}{2}=\sum_{n=1}^{\infty}B_nL_{mn}, \tag{4.52}$$

which leads to

$$A_m=-F\delta_{m1}+\frac{2}{\epsilon_m}\sum_{n=1}^{\infty}B_nL_{mn}, \tag{4.53}$$

Where $\epsilon_n=2$ if $n=0$ and $n=1$ otherwise

$$L_{mn}=\int_0^d Y_{1n}(y)\cos(m\pi y)dy+\int_d^1 Y_{2n}(y)\cos(m\pi y)dy. \tag{4.54}$$

Continuity of Normal Velocity

$$\psi_{2x}(0,y)=\psi_{1x}(0,y),$$

using (4.7) and (4.27), we get

$$i\sum_{n=1}^{\infty}B_ns_nY_n=i\eta_1F\cos(\pi y)-i\sum_{n=0}^{\infty}A_n\eta_n\cos(n\pi y). \tag{4.55}$$

Multiply (4.55) with $Y_j(y)$ and integrate 0 to d and d to 1, we get

$$\sum_{n=1}^{\infty} B_n s_n \int_0^d Y_{1n} Y_{1j} dy + \int_d^1 Y_{2n} Y_{2j} dy = \eta_1 F \int_0^d \cos(\pi y) Y_{1j} dy + \int_d^1 \cos(\pi y) Y_{2j} dy$$
$$- \sum_{0}^{\infty} A_n \eta_n \int_0^d Y_{1j} \cos(n\pi y) + \int_d^1 Y_{2j} \cos(n\pi y). \tag{4.56}$$

On using orthogonality relation (4.28) and (4.29), we get

$$\sum_{n=1}^{\infty} B_n s_n \delta_{jn} P_j = \eta_1 F L_{1j} - \sum_{n=1}^{\infty} A_n \eta_n L_{nj}, \tag{4.57}$$

which leads to

$$B_j = \frac{\eta_1 F L_{1j}}{s_j P_j} - \frac{1}{s_j P_j} \sum_{n=1}^{\infty} A_n \eta_n L_{nj}, \quad j \geq 1. \tag{4.58}$$

Now using (4.53) into (4.58), we found

$$B_j = \frac{\eta_1 F L_{1j}}{s_j P_j} - \frac{1}{s_j P_j} \sum_{n=1}^{\infty} \left(\frac{-2F\delta_{n0}}{\epsilon_n} + \frac{2}{\epsilon_n} \sum_{m=1}^{\infty} B_n L_{nm} \right) \eta_n L_{nj}, \tag{4.59}$$

which on simplification leads to

$$B_j = \frac{2\eta_1 F L_{1j}}{s_j P_j} - 2 \sum_{n=0}^{\infty} \frac{B_n}{s_j P_j} \sum_{m=0}^{\infty} \frac{\eta_m}{\epsilon_m} L_{mj} L_{mn}. \tag{4.60}$$

For $J \geq 1$, we have

$$B_j \sqrt{s_j P_j} = \frac{2\eta_1 F L_{1j}}{\sqrt{s_j P_j}} - 2 \sum_{n=0}^{\infty} \frac{b_n}{\sqrt{s_n P_n}} \frac{1}{\sqrt{s_j P_j}} \sum_{m=0}^{\infty} \frac{\eta_m}{\epsilon_m} L_{mj} L_{mn}, \tag{4.61}$$

or

$$b_j = \frac{2\eta_1 F L_{1j}}{\sqrt{s_j P_j}} - 2 \sum_{n=0}^{\infty} b_n S_{jn}, j \geq 1, \tag{4.62}$$

where

$$S_{jn} = \frac{1}{\sqrt{s_j s_n P_j P_n}} \sum_{m=0}^{\infty} \frac{\eta_m}{\epsilon_m} L_{mj} L_{mn}, \tag{4.63}$$

and $b_n = B_n \sqrt{s_n P_n}$, n=1,2,3,$\cdots$.

4.4 Enhanced Mode-Matching Solution with Two Exceptional Points

At the EP_2 point, the double root of the equation $K(s) = 0$ occurs at α_1, leading to a zero derivative $K'(s_1) = 0$ and consequently $P_1 = 0$. This results in $Y_1(y)$ being self-orthogonal, causing the systems of equations (4.53) and (4.58) to become degenerate. To simplify the structure of the EP_2 eigenfunction expansion, it's beneficial to express the waveform in terms of functions that depend on y and their derivatives, making the formulation more straightforward. This done by using (4.25), we have

$$Y_1' = \frac{\partial Y_1}{\partial s} = \frac{\partial Y_1}{\partial \alpha_1}.\frac{\partial \alpha_1}{\partial s_1}, \tag{4.64}$$

using (4.25), we have

$$\frac{\partial Y_1}{\partial s} = -y\sin(\alpha y)\frac{-s_1}{\alpha_1}. \tag{4.65}$$

Now on using (4.25) to eliminate $\sin\alpha_1 y$, we found

$$Y_1' = \chi_1(y), \tag{4.66}$$

where

$$\chi_1(y) = -\frac{s_1 y}{\alpha_1^2}\frac{\partial Y_1}{\partial y}, \tag{4.67}$$

Now for Y_2' again using (4.25), we get

$$Y_2' = \frac{\partial Y_2}{\partial s} = \frac{\partial Y_2}{\partial \alpha_1}.\frac{\partial \alpha_1}{\partial s_1}, \tag{4.68}$$

or

$$\frac{\partial Y_2}{\partial s} = \left(\frac{-s_1}{\alpha_1}\frac{\sin(\alpha_1 d)}{\sin\alpha_1(d-1)}\right)(-(y-1)\sin\alpha_1(y-1)) - \frac{-s_1}{\alpha_1}\cos\alpha_1(y-1)$$
$$\left(\frac{d\cos(\alpha_1 d)\sin\alpha_1(d-1) - (d-1)\sin(\alpha_1 d)\cos\alpha_1(d-1)}{\sin^2\alpha_1(d-1)}\right), \tag{4.69}$$

here for simplification we have to find the derivative of Y_2 with respect to y. so using (4.25), we get

$$\frac{\partial Y_2}{\partial y} = \frac{-\alpha_1 \sin(\alpha_1 d)}{\sin \alpha_1(d-1)} \sin \alpha_1(y-1), \tag{4.70}$$

using (4.70) into (4.69) we found

$$\frac{\partial Y_2}{\partial s} = \frac{-s_1}{\alpha^2}\frac{\partial Y_2}{\partial y}(y-1) + \frac{s_1}{\alpha_1}\frac{d\cos\alpha(y-1)\sin\alpha}{\sin^2\alpha(d-1)} - \frac{s_1}{\alpha_1}\frac{\cos\alpha_1(d-1)Y_2}{\sin\alpha(d-1)} \tag{4.71}$$

We have to find $\sin\alpha$ as K(s)=0 using (4.24) we get

$$\frac{\partial Y_2}{\partial s} = \frac{-s_1}{\alpha_1^2}\frac{\partial Y_2}{\partial y}(y-1) - iCs_1 dY_2 - \frac{s_1}{\alpha_1}\frac{\cos\alpha_1(d-1)Y_2}{\sin\alpha_1(d-1)} \tag{4.72}$$

by little manipulation,

$$\frac{\partial Y_2}{\partial s} = \chi_2(y) \tag{4.73}$$

where

$$\sin\alpha_1 = -iC\alpha_1 \sin(\alpha_1 d)\sin\alpha_1(d-1),$$

and

$$\chi_2(y) = \frac{-s_1}{\alpha_1^2}\frac{\partial Y_2}{\partial y}(y-1) - iCsdY_2 - \frac{s_1}{\alpha_1}\cot\alpha_1(d-1)Y_2.$$

Thus at EP_2 ψ_2 take the form:

$$\psi_2 = \bar{B_1}\begin{cases}[\chi_1(y) + ixY_1(y)]e^{is_1x} & 0<y<d \\ [\chi_2(y) + ixY_2(y)]e^{is_1x} & d<y<1\end{cases} + \sum_{n=1}^{\infty} B_n Y_n e^{is_n x}, \tag{4.74}$$

and

$$\int_0^d \chi_1(y)Y_{1n}(y)dy + \int_d^1 \chi_2(y)Y_{2n}(y)dy = Q\delta_{1n}, \tag{4.75}$$

it is further worth noting that $Q = 0$ at EP_3.

Continuity of Pressure

$$\psi_1(0,y) = \psi_2(0,y), \quad 0 < y < 1,$$

using (4.7) and (4.74), in (4.49) we get

$$F\cos(\pi y) + \sum_{n=0}^{\infty} A_n \cos(n\pi y) = \bar{B}_1 \begin{cases} \chi_1(y) & 0 < y < d \\ \chi_2(y) & d < y < 1 \end{cases} + \sum_{n=1}^{\infty} B_n Y_n(y). \quad (4.76)$$

Multiply (4.76) with $\cos(m\pi y)$ and integrating from 0 to d and d to 1

$$\begin{aligned} & F\left[\int_0^d \cos(\pi y)\cos(m\pi y)dy + \int_d^1 \cos(\pi y)\cos(m\pi y)dy\right] \\ & + \sum_{n=0}^{\infty} A_n \left[\int_0^d \cos(m\pi y)\cos(n\pi y)dy + \int_d^1 \cos(m\pi y)\cos(n\pi y)dy\right] \\ & = \bar{B}_1 \left[\int_0^d \cos(m\pi y)\chi_1(y)dy + \int_d^1 \cos(m\pi y)\chi_2(y)dy\right] \\ & + \sum_{n=1}^{\infty} B_n \left[\int_0^d \cos(m\pi y)Y_{1n}(y)dy + \int_d^1 \cos(m\pi y)Y_{2n}(y)dy\right], \end{aligned} \quad (4.77)$$

which leads to

$$F\delta_{m1}\frac{\epsilon_m}{2} + \sum_{n=0}^{\infty} A_n \delta_{mn}\frac{\epsilon_m}{2} = \bar{B}_1 M_m + \sum_{n=1}^{\infty} B_n L_{mn}, \quad (4.78)$$

where

$$M_m = \left[\int_0^d \cos(m\pi y)\chi_1(y)dy + \int_d^1 \cos(m\pi y)\chi_2(y)dy\right], \quad (4.79)$$

$$A_m = -F\delta_{m1} + \frac{2}{\epsilon_m}\bar{B}_1 M_m + \frac{2}{\epsilon_m}\sum_{n=1}^{\infty} B_n L_{mn}. \quad (4.80)$$

Continuity of Normal Velocity

$$\psi_{2x}(0,y) = \psi_{1x}(0,y),$$

using (4.7) and (4.74), we get

$$i\sum_{n=1}^{\infty} B_n s_n Y_n = i\eta_1 F\cos(\pi y) - i\sum_{n=0}^{\infty} A_n \eta_n \cos(n\pi y). \quad (4.81)$$

Multiply (4.84) through $Y_j(y)$ and integrate 0 to 1

$$\begin{aligned}
&\eta_1 F\left[\int_0^d \cos(\pi y)Y_{1j}dy + \int_d^1 \cos(\pi y)Y_{2j}dy\right] \\
&-\sum_{n=0}^{\infty} A_n\eta_n\left[\int_0^d Y_{1j}\cos(n\pi y) + \int_d^1 Y_{2j}\cos(n\pi y)\right] \\
&=\sum_{n=1}^{\infty} B_n s_n\left[\int_0^d Y_{1n}Y_{1j}dy + \int_d^1 Y_{2n}Y_{2j}dy\right],
\end{aligned} \tag{4.82}$$

which leads to

$$\sum_{n=1}^{\infty} B_n s_n \delta_{jn} P_j = \eta_1 F L_{1j} - \sum_{n=1}^{\infty} A_n\eta_n L_{nj}, \tag{4.83}$$

or

$$B_j = \frac{\eta_1 F L_{1j}}{s_j P_j} - \frac{1}{s_j P_j}\sum_{n=1}^{\infty} A_n\eta_n L_{nj}, \quad j \geq 1. \tag{4.84}$$

Since $Y_1(y)$ is self orthogonal for $j \geq 1$ and have no information about B and $\bar{B}$. Thus, there are two additional equation for B and $\bar{B}$ in (4.74), so using conditions of normal velocity we get

$$\begin{aligned}
\bar{B}_1\begin{cases}[\chi_1(y)+Y_1(y)] & 0<y<d \\ [\chi_2(y)+Y_2(y)] & d<y<1\end{cases} + B_1\begin{cases}Y_1(y)s_1 & 0<y<d \\ Y_2(y)s_1 & d<y<1\end{cases} \\
= \eta_1 F\cos(\pi y) - \sum_{n=0}^{\infty} A_n\eta_n\cos(n\pi y).
\end{aligned} \tag{4.85}$$

Multiply (4.85) with Y_1 and Y_2 and integrate 0 to d and d to 1 respectively

$$\begin{aligned}
&\bar{B}_1 s_1\left[\int_0^d \chi_1(y)Y_1dy + \int_d^1 \chi_2(y)Y_2dy\right] + \bar{B}_1\left[\int_0^d Y_1^2dy + \int_d^1 Y_2^2dy\right] \\
&+ B_1 s_1\left[\int_0^d Y_1^2dy + \int_d^1 Y_2^2dy\right] = \eta_1 F\left[\int_0^d \cos(\pi y)Y_1dy + \int_d^1 \cos(\pi y)Y_2dy\right] \\
&-\sum_{n=0}^{\infty} A_n\eta_n\left[\int_0^d \cos(n\pi y)Y_1dy + \int_d^1 \cos(n\pi y)Y_2dy\right],
\end{aligned} \tag{4.86}$$

which on simplification leads to

$$\bar{B}_1 s_1 Q = \eta_1 F L_{11} - \sum_{n=0}^{\infty} A_n \eta_n L_{n1}. \tag{4.87}$$

Now multiply (4.85) with $\chi(y)$ and integrate 0 to d and d to 1 respectively

$$\begin{aligned}
&\bar{B}_1 s_1 \left[\int_0^d \chi_1^2(y)dy + \int_d^1 \chi_2^2(y)dy\right] - \bar{B}_1 \left[\int_0^d Y_1\chi_1(y)dy + \int_d^1 Y_2\chi_2(y)dy\right] \\
&+ B_1 s_1 \left[\int_0^d Y_1\chi_1(y)dy + \int_d^1 Y_2\chi_2(y)dy\right] \\
&= \eta_1 F \left[\int_0^d \cos(\pi y)\chi_1(y)dy + \int_d^1 \cos(\pi y)\chi_2(y)dy\right] \\
&- \sum_{n=0}^{\infty} A_n \eta_n \left[\int_0^d \cos(n\pi y)\chi_1(y)dy + \int_d^1 \cos(n\pi y)\chi_2(y)dy\right],
\end{aligned} \tag{4.88}$$

which leads to

$$\bar{B}_1 s_1 T - \bar{B}_1 Q + B_1 s_1 Q = \eta_1 F M_1 - \sum_{n=0}^{\infty} A_n \eta_n M_n. \tag{4.89}$$

Now combining (4.87) and (4.89), we get

$$\begin{pmatrix} s_1 Q & s_1 T - Q \\ 0 & s_1 Q \end{pmatrix} \begin{pmatrix} B_1 \\ \bar{B}_1 \end{pmatrix} = \begin{pmatrix} \eta_1 F M_1 - \sum_{n=0}^{\infty} A_n \eta_n M_n \\ \eta_1 F L_{11} - \sum_{n=0}^{\infty} A_n \eta_n L_{n1} \end{pmatrix}, \tag{4.90}$$

where

$$T = \left[\int_0^d \chi_1^2(y)dy + \int_d^1 \chi_2^2(y)dy\right]. \tag{4.91}$$

4.5 Numerical Results

The numerical results demonstrate a high degree of accuracy and consistency across the different regions of the fluid, confirming the effectiveness of the truncated solution approach in capturing the physical behavior of the system. The graphs show a very good match between the predicted pressures and velocities in the fluid areas. This means that the simplified solution is accurate and effectively

combines the different regions together. The excellent match confirms that the numerical method is reliable and produces trustworthy results. Here we truncate the system by taking m=n=0,1,2,...,N and the numerical calculations are carried out using the software MATHEMATICA, where the relevant parameters are set to specific values. By solving these equations, we obtain the coefficients An, B_n, $n = 0, 1, 2, \cdots, N$.

Once these scattered coefficients are known the pressures and velocities can be plotted at interface. To display the graphs, we fixed the height of the ducts at $h_1 = 0.25m$ and $h_2 = 0.35m$, $c = 343.5m/s$ and $a = 1$. The graphs illustrate the variation in pressure and velocity components as a function of duct height, normalized to a reference point at the interface where the ducts connect in figures 4.2-4.5.

The physical parameters from figure 4.2-4.5 are $f = 500$, $T = 124N$, $C = 0.476066$ and $N = 30$ terms. The physical parameters from figure 4.6-4.9 are $f = 1000$, $T = 124N$, $C = 0.476066$ and $N = 30$ terms.

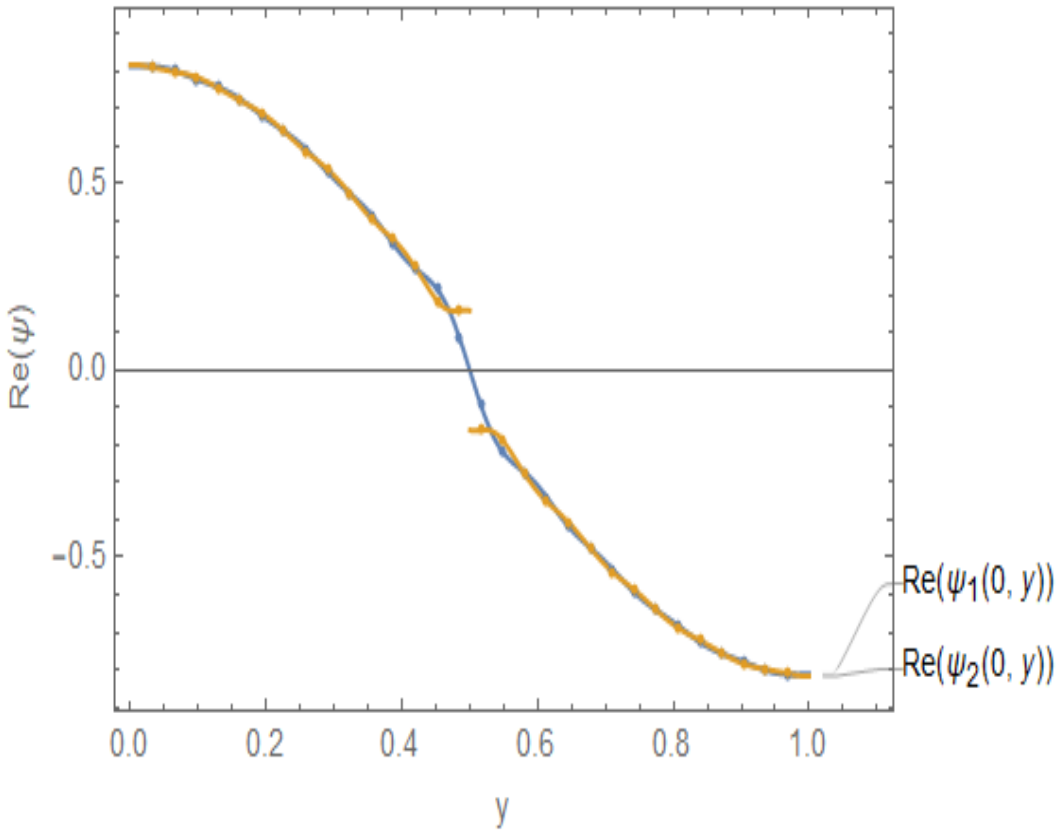

FIGURE 4.2: Real part of pressures $\psi_1(0, y)$ and $\psi_2(0, y)$

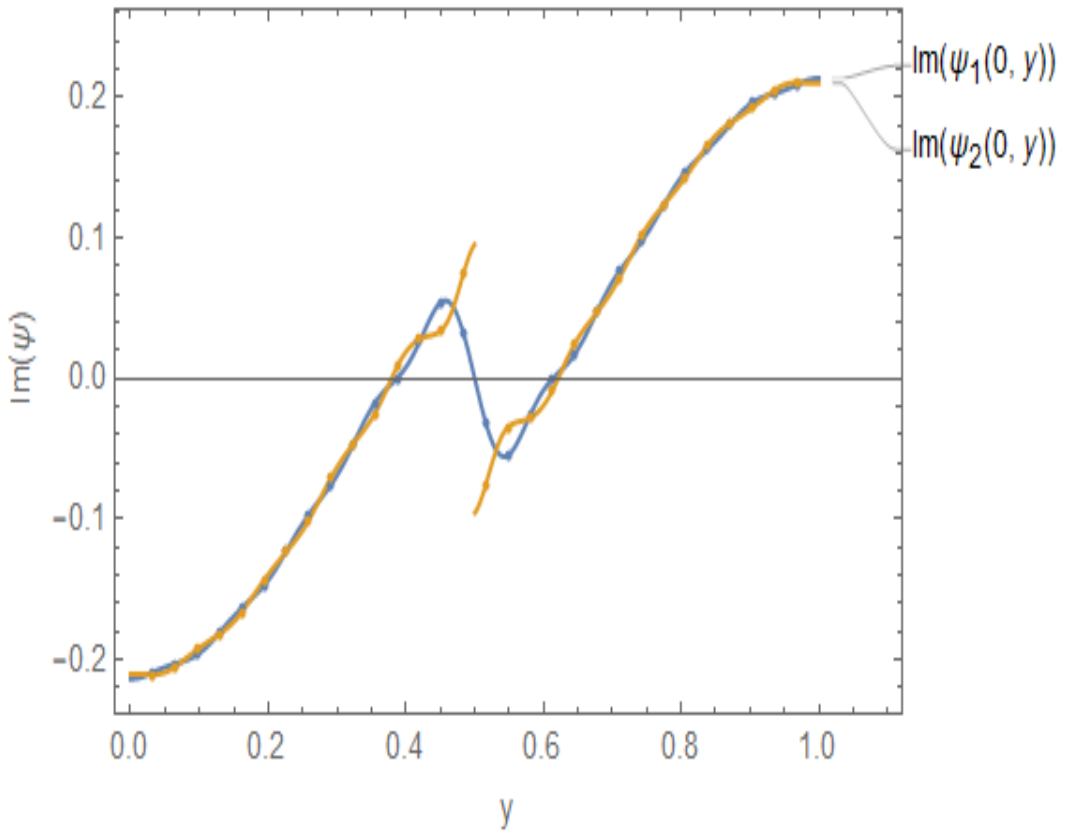

FIGURE 4.3: Imaginary part of pressures $\psi_1(0, y)$ and $\psi_2(0, y)$.

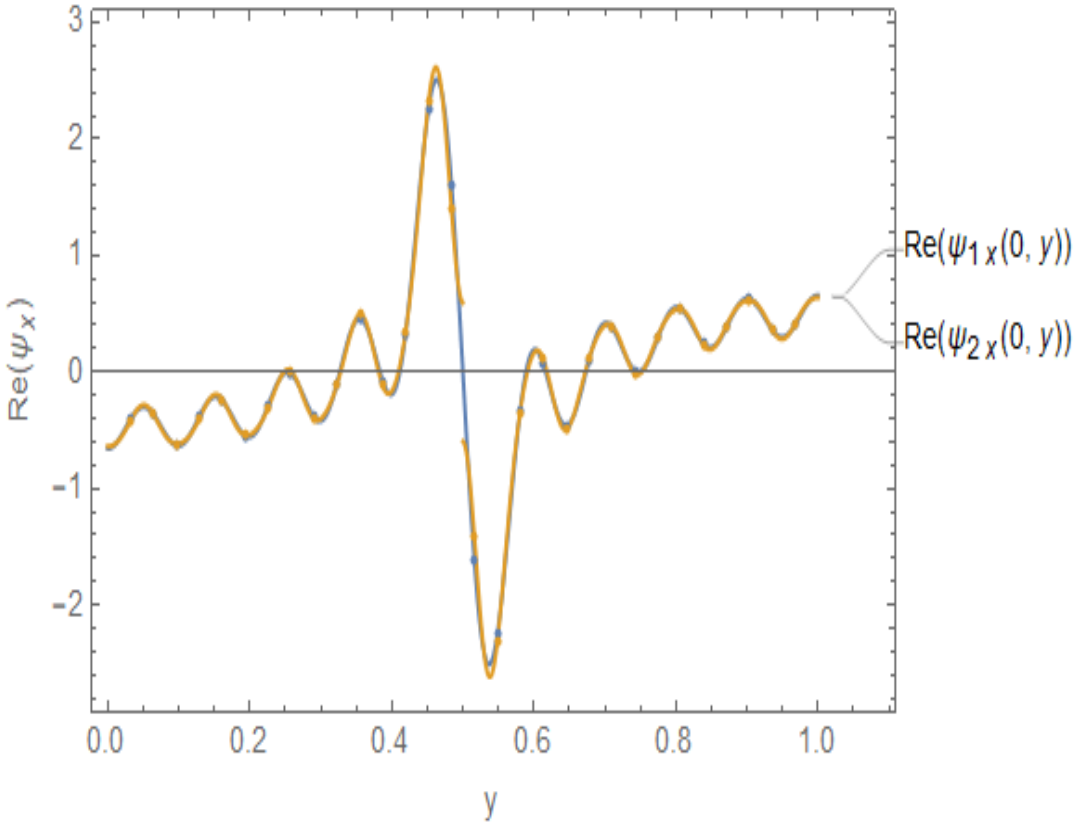

FIGURE 4.4: Real part of velocities $\psi_{1x}(0, y)$ and $\psi_{2x}(0, y)$.

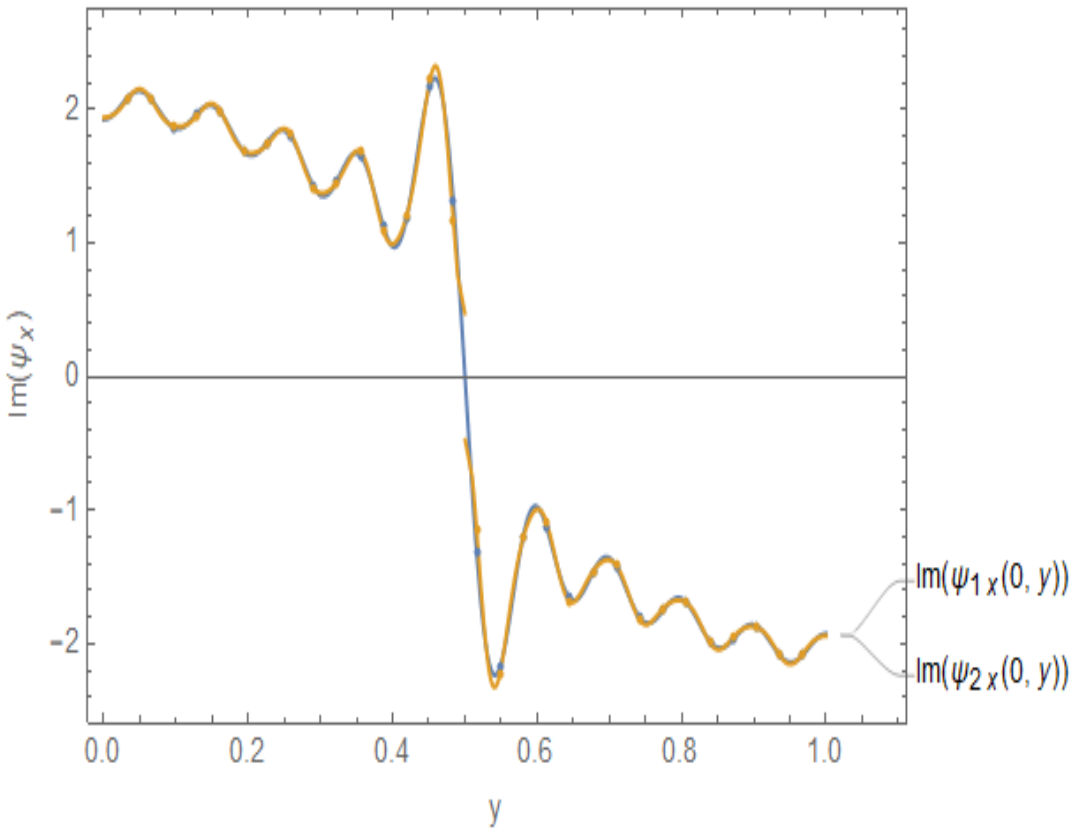

FIGURE 4.5: Imaginary part of velocities $\psi_{1x}(0, y)$ and $\psi_{2x}(0, y)$.

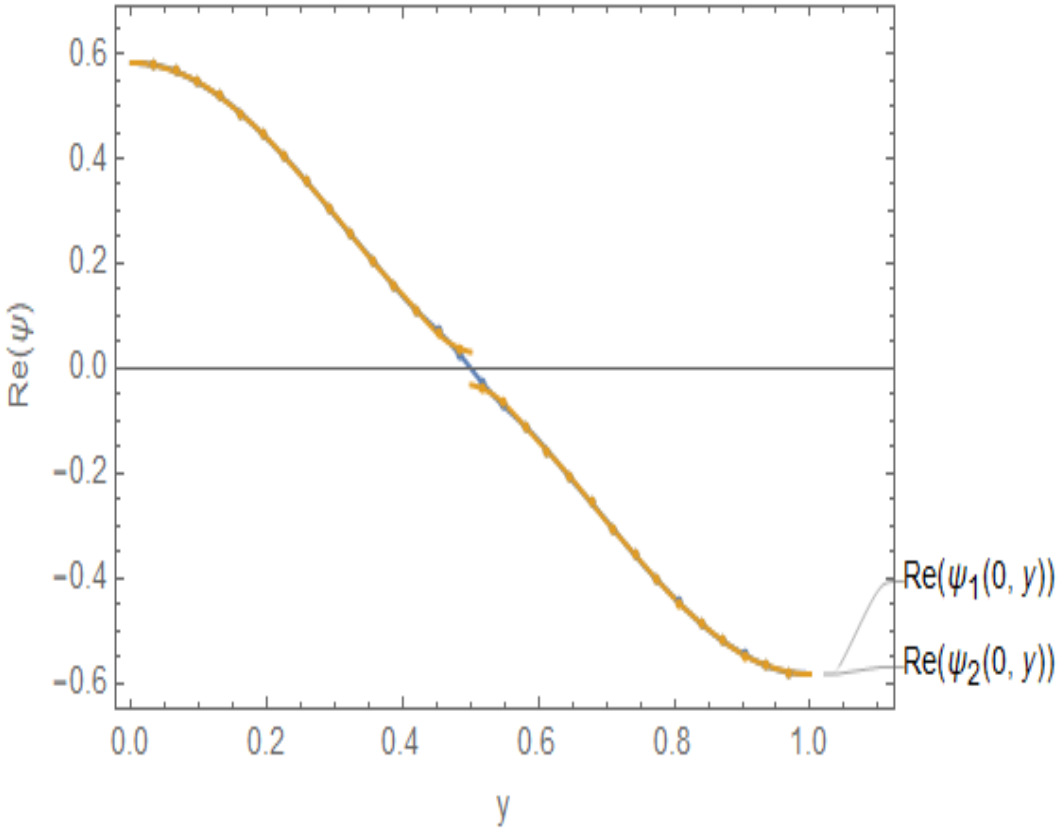

FIGURE 4.6: Real part of pressures $\psi_1(0, y)$ and $\psi_2(0, y)$

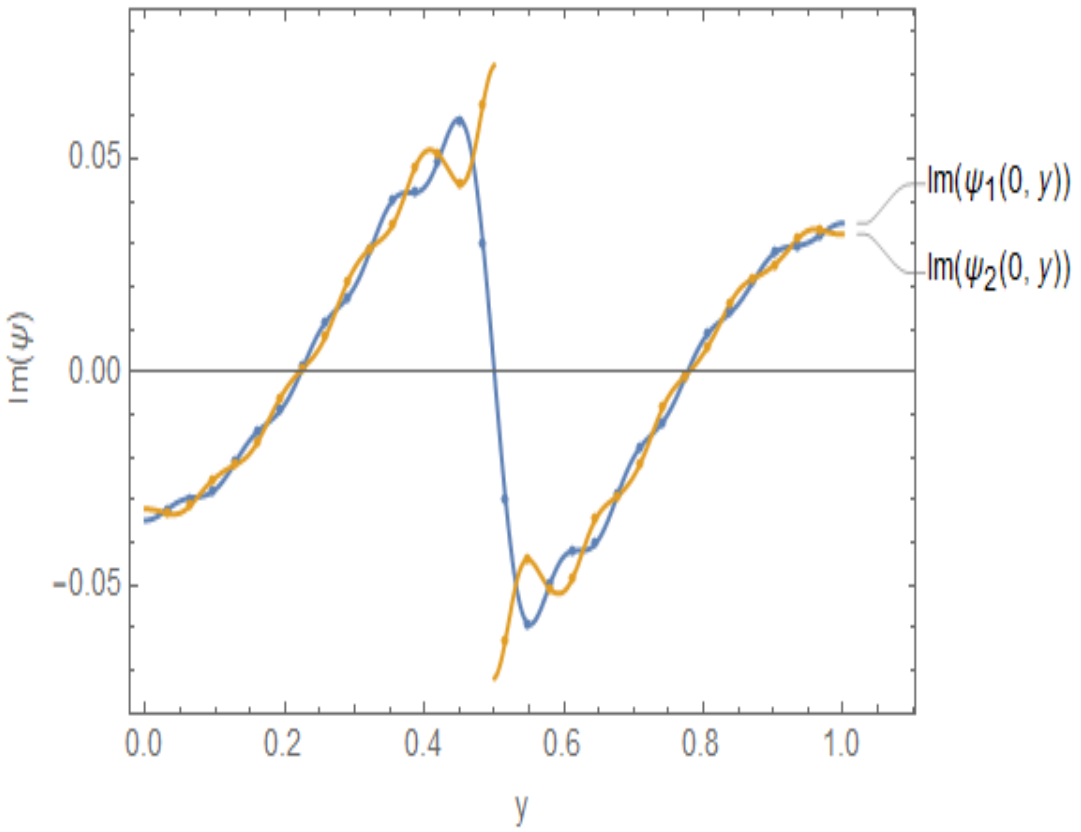

FIGURE 4.7: Imaginary part of pressures $\psi_1(0, y)$ and $\psi_2(0, y)$.

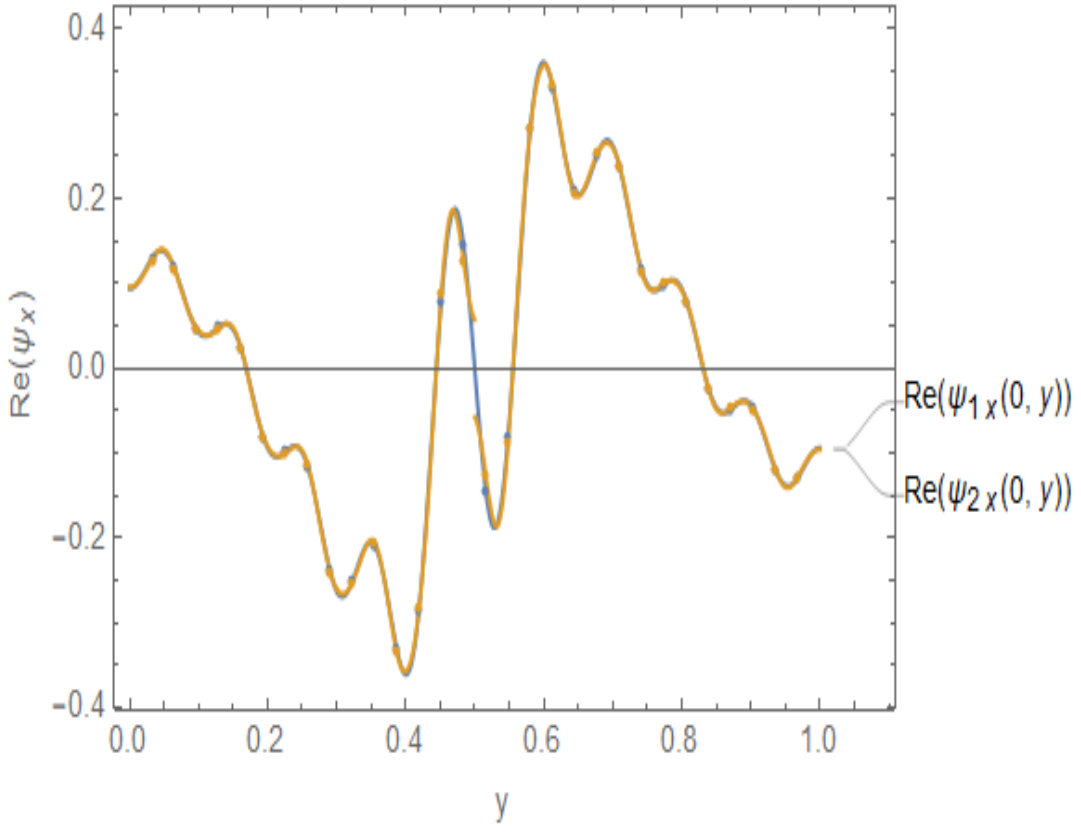

FIGURE 4.8: Real part of velocities $\psi_{1x}(0, y)$ and $\psi_{2x}(0, y)$.

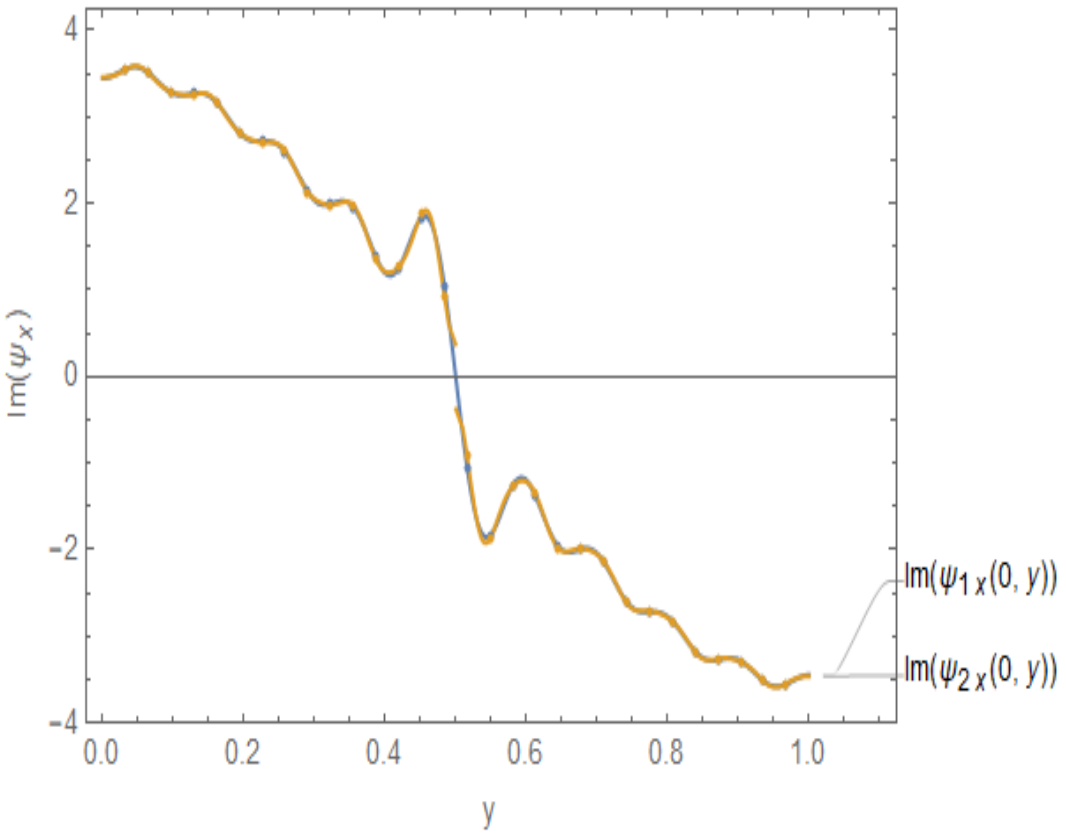

FIGURE 4.9: Imaginary part of velocities $\psi_{1x}(0, y)$ and $\psi_{2x}(0, y)$.

Figs. 4.2,4.3 and 4.6,4.7 show the real and imaginary parts of pressure $\psi_1(0, y)$ and $\psi_2(0, y)$ in the regions $0 \leq y \leq h_1$ and $0 \leq y \leq h_2$, respectively. The real and imaginary parts of normal velocities $\psi_{1x}(0, y)$ and $\psi_{2x}(0, y)$ for the respective regions are plotted in Figs. 4.4,4.5 and 4.8,4.9. Matching conditions are satisfied according to the problem. Although the values of gamma are taken by using a different algorithm. The graphs show a very good match between the predicted pressures and velocities in the fluid areas. This means that the simplified solution is accurate and effectively combines the different regions together. The excellent match confirms that the numerical method is reliable and produces trustworthy results.

Chapter 5

Summary and Conclusion

The chapter wise summary and conclusion of the present study are enclosed in this chapter. **Chapter 1** contains background and literature review to the current study along with thesis structure. This thesis presents a comprehensive analysis of acoustic wave propagation in lined waveguides, including:

- A detailed exposition of the analytical mode-matching technique
- A brief overview of the accurate handling of exceptional points in lined acoustic waveguides
- An investigation of wave propagation through modes in a waveguide with an embedded wire mesh

The thesis provides a thorough understanding of the modal behavior and exceptional points in such systems, offering insights into the effects of wire mesh embedded in the waveguide on wave propagation.
In **chapter 2** we have discussed some basic definitions which are useful in understanding the mathematical modeling and associated physical characteristics of the work presented in the rest of the chapters.
Chapter 3 explores the fundamental development of a canonical problem in acoustic wave propagation. A plane acoustic wave propagates from a rigid duct into a

duct lined with sound-absorbing material, creating an interface between the two sections. The goal is to find out the resulting reflected and transmitted sound fields, analyzing how the acoustic wave interacts with the interface and the absorbing material. Additionally, the chapter explore the concept of exceptional points EP_s and employs a mode-matching scheme to address them. Specifically, a standard analytical mode-matching approach is used for cases without EP_s, while an extended mode-matching scheme, incorporating additional wave forms, is developed to tackle cases with two (EP_2) and three (EP_3) exceptional points.

Chapter 4 examines the propagation of waves through modes in a waveguide with an embedded wire mesh. The insertion of a wire mesh parallel to the waveguides walls is a effective approach for optimizing modal attenuation. By strategically placing the wire mesh at a critical location, it is possible to achieve Exceptional Points EP_s for the first two higher order modes, leading to enhanced modal attenuation and control over wave propagation. The chapter begins by deriving the dispersion relation for transverse modes, which are governed by Helmholtz's equation and subject to rigid and lined boundary conditions. The mode-matching method is then employed to solve the boundary value problem, leveraging its convenience and orthogonality relations for the coupled equations. Notably, it is found that mode 0 remains unaffected by the wiremesh in the absence of Exceptional Points EP_s. A multi-mode solution is derived by projecting local transverse modes onto the coupled equations, effectively decomposing the solution into multiple modes that capture the complex behavior of the system.

The enhanced mode-matching scheme is tested and works well, showing it can be used to solve many different types of complex problems. And the numerical results demonstrate a high degree of accuracy and consistency across the different regions of the fluid, confirming the effectiveness of the truncated solution approach in capturing the physical behavior of the system. The matching conditions, which ensure the continuity of physical quantities across interfaces, are well-satisfied, further validating the results.

Bibliography

[1] Mats Åbom and Stefan Jacob. A comment on the correct boundary conditions for the cremer impedance. *JASA Express Letters*, 1(2), 2021.

[2] Muhammad Afzal and Hazrat Bilal. Acoustic wave scattering from a wave-bearing cavity in a rectangular waveguide. *The Journal of the Acoustical Society of America*, 144(3_Supplement):1681–1681, 2018.

[3] Muhammad Afzal, Tahir Nawaz, and Rab Nawaz. Scattering characteristics of planar trifurcated waveguide structure containing multiple discontinuities. *Waves in Random and Complex Media*, 32(6):2776–2795, 2022.

[4] Muhammad Afzal, Junaid Uzair Satti, and Rab Nawaz. Scattering characteristics of non-planar trifurcated waveguides. *Meccanica*, 55(5):977–988, 2020.

[5] Muhammad Afzal and Sajid Shafique. Attenuation analysis of flexural modes with absorbent lined flanges and different edge conditions. *The Journal of the Acoustical Society of America*, 148(1):85–99, 2020.

[6] Muhammad Afzal, Sajid Shafique, and Abdul Wahab. Analysis of traveling waveform of flexible waveguides containing absorbent material along flanged junctions. *Communications in Nonlinear Science and Numerical Simulation*, 97:105737, 2021.

[7] Yuto Ashida, Zongping Gong, and Masahito Ueda. Non-hermitian physics. *Advances in Physics*, 69(3):249–435, 2020.

[8] Emil J Bergholtz, Jan Carl Budich, and Flore K Kunst. Exceptional topology of non-hermitian systems. *Reviews of Modern Physics*, 93(1):015005, 2021.

[9] Wenping Bi and Vincent Pagneux. New insights into mode behaviours in waveguides with impedance boundary conditions. *arXiv preprint arXiv:1511.05508*, 2015.

[10] Edward J Brambley and Nigel Peake. Classification of aeroacoustically relevant surface modes in cylindrical lined ducts. *Wave motion*, 43(4):301–310, 2006.

[11] Lothar Cremer. Theory regarding the attenuation of sound transmitted by air in a rectangular duct with an absorbing wall, and the maximum attenuation constant produced during this process. *Acustica*, 3(1):249–263, 1953.

[12] M Farooqui, Yves Aurégan, and V Pagneux. Ultrathin resistive sheets for broadband coherent absorption and symmetrization of acoustic waves. *Physical Review Applied*, 18(1):014007, 2022.

[13] Tamar Goldzak, Alexei A Mailybaev, and Nimrod Moiseyev. Light stops at exceptional points. *Physical review letters*, 120(1):013901, 2018.

[14] Eva-Maria Graefe and HF Jones. Pt-symmetric sinusoidal optical lattices at the symmetry-breaking threshold. *Physical Review A*, 84(1):013818, 2011.

[15] Wei Guo, Juan Liu, Wenping Bi, Desen Yang, Yves Aurégan, and Vincent Pagneux. Spatial transient behavior in waveguides with lossy impedance boundary conditions. *arXiv preprint arXiv:2010.03646*, 2020.

[16] Lixi Huang. Modal analysis of a drumlike silencer. *the Journal of the Acoustical Society of America*, 112(5):2014–2025, 2002.

[17] Matthew Kelsten. *Modeling of acoustic waves in pipes with impedance walls and double roots*. PhD thesis, Rutgers University-School of Graduate Studies, 2018.

[18] Lawrence E Kinsler, Austin R Frey, Alan B Coppens, and James V Sanders. *Fundamentals of acoustics*. John wiley & sons, 2000.

[19] Alex Krasnok, Denis Baranov, Huanan Li, Mohammad-Ali Miri, Francesco Monticone, and Andrea Alú. Anomalies in light scattering. *Advances in Optics and Photonics*, 11(4):892–951, 2019.

[20] Svetlana Kuznetsova, Yves Aurégan, and Vincent Pagneux. Higher-order mode filtering by a resistive layer. *JASA Express Letters*, 3(10), 2023.

[21] Jane B Lawrie. Comments on a class of orthogonality relations relevant to fluid-structure interaction. *Journal of Engineering Mathematics*, 2012.

[22] Jane B Lawrie and Muhammad Afzal. Acoustic scattering in a waveguide with a height discontinuity bridged by a membrane: a tailored galerkin approach. *Journal of Engineering Mathematics*, 105:99–115, 2017.

[23] Jane B Lawrie and Ray Kirby. On analysing the performance of a dissipative silencer: a mode-matching approach. In *IUTAM Symposium on Asymptotics, Singularities and Homogenisation in Problems of Mechanics: Proceedings of the IUTAM Symposium held in Liverpool, United Kingdom, 8–11 July 2002*, pages 169–178. Springer, 2003.

[24] Jane B Lawrie and Ray Kirby. Mode-matching without root-finding: Application to a dissipative silencer. *The Journal of the Acoustical Society of America*, 119(4):2050–2061, 2006.

[25] Jane B Lawrie, Benoit Nennig, and E Perrey-Debain. Analytic mode-matching for accurate handling of exceptional points in a lined acoustic waveguide. *Proceedings of the Royal Society A*, 478(2268):20220484, 2022.

[26] Stefano Longhi. Spectral singularities and bragg scattering in complex crystals. *Physical Review A*, 81(2):022102, 2010.

[27] Konstantinos G Makris, Li Ge, and HE Türeci. Anomalous transient amplification of waves in non-normal photonic media. *Physical Review X*, 4(4):041044, 2014.

[28] Fariha Mir and Sourav Banerjee. Performance of a multifunctional spiral shaped acoustic metamaterial with synchronized low-frequency noise filtering and energy harvesting capability. In *Smart Materials, Adaptive Structures and Intelligent Systems*, volume 84027, page V001T01A006. American Society of Mechanical Engineers, 2020.

[29] Mohammad-Ali Miri and Andrea Alu. Exceptional points in optics and photonics. *Science*, 363(6422):eaar7709, 2019.

[30] Philip M Morse. The transmission of sound inside pipes. *The Journal of the Acoustical Society of America*, 11(2):205–210, 1939.

[31] Rab Nawaz, Aasim Ullah Jan, and Muhammad Afzal. Fluid-structure coupled wave scattering in a flexible duct at the junction of planar discontinuities. *Advances in Mechanical Engineering*, 9(7):1687814017713187, 2017.

[32] Touqeer Nawaz, Muhammad Afzal, and Rab Nawaz. The scattering analysis of trifurcated waveguide involving structural discontinuities. *Advances in Mechanical Engineering*, 11(7):1687814019829282, 2019.

[33] Touqeer Nawaz, Muhammad Afzal, and Abdul Wahab. Scattering analysis of a flexible trifurcated lined waveguide structure with step-discontinuities. *Physica Scripta*, 96(11):115004, 2021.

[34] Alessandro Orchini, Luca Magri, Camilo F Silva, Georg A Mensah, and Jonas P Moeck. Degenerate perturbation theory in thermoacoustics: high-order sensitivities and exceptional points. *Journal of Fluid Mechanics*, 903:A37, 2020.

[35] E Perrey-Debain, Benoit Nennig, and JB Lawrie. Mode coalescence and the green's function in a two-dimensional waveguide with arbitrary admittance boundary conditions. *Journal of Sound and Vibration*, 516:116510, 2022.

[36] Singiresu S Rao. *Vibration of continuous systems*. John Wiley & Sons, 2019.

[37] Sjoerd W Rienstra. A classification of duct modes based on surface waves. *Wave motion*, 37(2):119–135, 2003.

[38] Stefan Sack and Mats Åbom. Modal filters for mitigation of in-duct sound. In *Proceedings of Meetings on Acoustics*, volume 29. AIP Publishing, 2016.

[39] Junaid Uzair Satti, Muhammad Afzal, and Rab Nawaz. Scattering analysis of a partitioned wave-bearing cavity containing different material properties. *Physica Scripta*, 94(11):115223, 2019.

[40] AF Seybert, RA Seman, and MD Lattuca. Boundary element prediction of sound propagation in ducts containing bulk absorbing materials. *American Society of Mechanical Engineers*, 15328:101–108, 1998.

[41] Sajid Shafique, Muhammad Afzal, and Rab Nawaz. On the attenuation of fluid–structure coupled modes in a non-planar waveguide. *Mathematics and Mechanics of Solids*, 25(10):1831–1850, 2020.

[42] EL Shenderov. Helmholtz equation solutions corresponding to multiple roots of the dispersion equation for a waveguide with impedance walls. *Acoustical physics*, 46(3):357–363, 2000.

[43] George Gabriel Stokes. On the theories of the internal friction of fluids in motion, and of the equilibrium and motion of elastic solids. *Fluids*, 2007.

[44] BJ Tester. The optimization of modal sound attenuation in ducts, in the absence of mean flow. *Journal of Sound and Vibration*, 27(4):477–513, 1973.

[45] Zhe Zhang, Hans Bodén, and Mats Åbom. The cremer impedance: An investigation of the low frequency behavior. *Journal of Sound and Vibration*, 459:114844, 2019.